Molecular Characterization Of Plasma Membrane Organization During Early *Drosophila* Embryogenesis

Master's thesis (5th year)
2013-14

By

Tirthasree Das

20091048

BS-MS Dual Degree Program

Biology Division

Indian Institute of Science Education and Research (IISER)

Pune, India.

Thesis Guide: Dr. Richa Rikhy

Certificate

This is to certify that this dissertation entitled "**Molecular characterization of plasma membrane organization during early *Drosophila* embryogenesis**" towards the partial fulfillment of the BS-MS dual degree program at the Indian Institute of Science Education and Research, Pune represents original research carried out by **Tirthasree Das** at IISER Pune under the supervision of "Dr.Richa Rikhy, Assistant Professor, IISER Pune Biology Department" during the academic year 2013-2014.

Richa Rikhy

Assistant Professor

Biology Department

IISER Pune

Declaration

I hereby declare that the matter embodied in the report entitled **"Molecular characterization of plasma membrane organization during early *Drosophila* embryogenesis"** are the results of the investigations carried out by me at the Department of Biology, Indian Institute of Science Education and Research (IISER), Pune, under the supervision of **Dr.Richa Rikhy** and the same has not been submitted elsewhere for any other degree.

Tirthasree Das

Registration number- 20091048

BS-MS Dual Degree Student

IISER Pune

(2013-2014)

Abstract

Metazoan embryo development starts with division of a simple cell to epithelial cells containing a predominant hexagonal organization. Epithelial cells have distinct morphology and protein complexes demarcating the apical, lateral and basal domains. *Drosophila* embryogenesis is used as a model system to study the onset of this polarity and epithelial sheet organization. The plasma membrane (PM) of the syncytial embryo shows a microvillus contained apical domain and junctional protein contained lateral domain even before the formation of complete cells. Using time-lapse confocal microscopy of fluorescently tagged transgenes, we have found an increased hexagonal organization in the PM similar to epithelial cells in the syncytial cycle 13. Junctional proteins, Cadherin and Bazooka are present in the lateral domain of the syncytial PM. Bazooka is distributed more on the edges of polygonal PM, while cytoskeletal remodeling proteins of the Septin family are predominantly present in the vertices. Photo bleaching experiments with Cadherin-GFP show that its movement is restricted within one edge and does not cross over to the neighboring edge of a polygon. Although a similar phenomenon is observed in the syncytium with the labeled trans-membrane protein, Toll-Venus, but in cellularization it moves freely across edges. To elucidate on the mechanism by which the lateral membrane, polygonal polarity and packing arises, embryos mutant for Cadherin, Bazooka and Peanut are being studied. Preliminary analysis with Cadherin mutant embryos shows loose PM organization along with compromised lateral membrane length. Packing analysis shows more pentagons instead of hexagons in syncytial cycle 13 implying a role for the protein in PM organization during *Drosophila* embryogenesis.

List Of Figures

Fig.6.2. Schematic of compartmentalized diffusion of proteins during syncytium.

List of Graphs and Tables

Acknowledgement

It is an immense pleasure to thank my mentor, **Dr. Richa Rikhy** for giving me this wonderful opportunity to work in her group for the last three years and introducing me to the fly as a model system as well as the microscopes. The endless number of fruitful discussions that I had with her over the years, be it significant or trivial, is truly invaluable. I do sincerely acknowledge her willingness to share new ideas, enthusiasm to initiate novel projects and determination to drive them to an end. This research experience is a foundation from which I have numerous lessons to carry forward with me and use them in my career as a researcher. I also owe my gratitude to Dr.Girish Ratnaparkhi for his helpful suggestions on this project.

I would like to profusely thank my lab mates Bipasha, Sameer, Aparna for their help with experiments, data analysis and valuable discussions on several occasions. I would deeply acknowledge their contribution for guiding me throughout the project and for planning, supporting and its implementation. I also thank my other lab members Darshika, Sayali, Dnyanesh and Prachi for being so friendly in the lab throughout. I thank my friends for all the time they spent with me whenever I felt like taking breaks from work and for their support in all the past five years.

The successful implementation of this project would not have been possible for me without the great scientific and learning environment provided by IISER Pune and the facilities of the Biology Department. I am also highly obliged by Kishore Vaigyanik Protsahan Yojana providing me stipend throughout my entire duration at IISER, Pune. Above all, I would like to thank my parents and family for their emotional support for last five years.

Introduction

Cell formation and origin of cell polarity

Embryo development across all kinds of multi-cellular organisms starts after the event of fertilization with the division of a single cell, giving rise to multiple cells after several rounds of cell division. Differentiation of these cells to different types eventually forms tissues and organs needed for the organism's proper functioning. Majority of the cells formed in the very first few divisions are polarized, which means that a single cell is subdivided into functionally and structurally distinct compartments. In general, this establishment of cell polarity involves molecular determinants that are asymmetrically localized either in the oocyte during maturation or upon fertilization. During division, these determinants are differentially segregated between daughter cells, and lineage commitment depends on the determinants that a daughter cell receives.

For example, in general, plant embryogenesis starts with a single-celled zygote undergoing an asymmetric cell division to give rise to a small apical cell which becomes an embryo and a large basal cell functioning to provide nutrients to the growing embryo. In *Arabidopsis thaliana,* it has been found that in addition to the external cues, this symmetry breaking event is triggered by the differential distribution of signaling components of MAPKKK pathway and the homeodomain transcription factor family proteins (WOX2 and WOX8) (Petricka et al., 2009). Similarly, in early C.*elegans* embryo development, after fertilization, the oocyte completes meiosis, following which the mitotic apparatus develops along the long axis of egg and migrates slightly to one end of the embryo (Rose and Kemphues, 1998). Polarization at this stage is due to retraction of actomyosin flow of cortical non muscle myosin (NMY-2) and F-actin towards the opposite future anterior pole(Munro et al., 2004). As a result of this asymmetry, the first cleavage division is unequal and produces larger anterior and smaller posterior cells due to segregation of PAR family of proteins(St Johnston and Ahringer, 2010). In another instance of polarity initiation, at the pre-implantation stage of mouse embryo development, 2-celled blastomeres exhibit polarized distribution of surface E-Cadherin at their contact sites (Neganova et al., 2000).

Inception of Polarity in the Plasma Membrane of Epithelial Cells

A basic feature of cell polarity is the asymmetric organization of its plasma membrane (Orlando and Guo, 2009). Any completely polarized epithelial cell has both the plasma membrane (PM) and the cytoskeleton directly beneath the PM, which show differences in their molecular composition and structural organization. The PM typically is compartmentalized into different domains namely, apical, lateral and basal domains (apical and baso-lateral domains shown in the Figure 1.1). This apico-basal polarity is important for the establishment of adhesive junctions and the formation of a diffusion barrier that prevents the movement of solutes across the epithelium. This asymmetry arises mainly due to differences in lipid and protein composition and their characteristic localization patterns throughout the PM. There are two layers of regulation to control such transport of protein complexes and their incorporation into the membrane. The first layer involves targeted delivery of proteins specifically sorted for their destined locations. And the second layer of regulation is through polarized tethering and docking of vesicles at specific domains of the PM. In this context, small signaling molecules like Rho GTPases and recycling endosomes are implicated to recruit and deliver core polarity proteins to lateral cell surfaces and initiate the formation of a polarized apical PM and thus establish epithelial cell polarity (Golachowska et al., 2010).

What are the molecular complexes involved in PM polarity initiation in epithelial cells?

From invertebrates to vertebrates, there is some consensus about the proteins known to be localized in the plasma membrane during establishment of polarity. In fruit flies, formation of spot adherens junctions, with proteins like Cadherin begin during epithelial cell formation (cellularization) and later when they coalesce, a junction belt (zonula adherens) is formed in the apical part of the lateral membrane. A more basal junction complex known as the septate junction (SJ) characterized by proteins like Claudin, Coracle is also formed at this time. Just apical to the *Drosophila* ZA lie the sub-apical region (SAR), which has an organizing role in epithelial polarization but is not known to function as a site of cell–cell junctions. Contrasting with *Drosophila*, vertebrate epithelial cells lack SJs and instead exhibit tight junctions (TJs), cell–cell adhesive structures that lie apical to the vertebrate ZA in a position analogous to the *Drosophila* SAR (Gibson

and Ã, 2003). Some of the molecular players establishing apical domain identity are the PDZ containing proteins like Par-6, Bazooka/Par-3 and aPKC. The second polarity protein complex that gets localized in the apical domain of PM includes Crumbs (Crb), Stardust (Sdt) and PatJ. Third, a group of proteins consisting of Dlg, Lethal giant larvae (Lgl), and Scribble (Scrib) localizes to the baso-lateral PM domain (Assémat et al., 2008).

How does the plasma membrane of epithelial get polarized?

Maintaining distinct PM domains in epithelial cells depends on mutually antagonistic interactions between the polarity complexes as shown in Figure 1.1. The Crumbs complex (Crumb/ Stardust/ PATJ), which is enriched immediately above where the tight junctions form, interacts with PAR-6 and atypical protein kinase C (aPKC) at the apical domain to exclude PAR-3 (Bazooka in *Drosophila*) and the Scribble complex. In turn, Scribble excludes aPKC at the lateral domain. These interactions may lead to the asymmetric distribution of phospholipids, i.e., phosphatidylinositide phosphates (PIPs), with PIP3 restricted to the baso-lateral membrane and PIP2 concentrated in the apical membrane. To help establish this asymmetry PTEN (phosphatase and tensin homolog) is localized to the apical junction by PAR-3 (Bazooka), where it converts PIP3 to PIP2. In addition, PI3-kinase (PI3K) may be recruited to the lateral membrane by Discs large (Dlg), where it creates PIP3 by phosphorylating PIP2 (St Johnston and Ahringer, 2010).

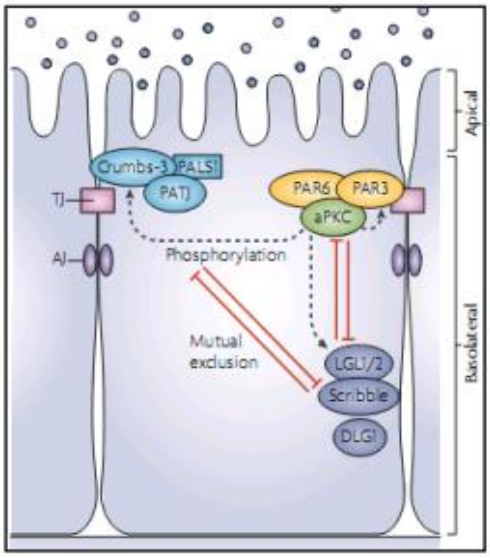

Fig.1.1 . Three conserved protein complexes — the partitioning defective (PAR), Crumbs and Scribble complexes — shows mutual antagonistic interaction for their polarized localization. Abbreviations: AJ (Adherens Junction) ; TJ (Tight Junction). (Ellenbroek et al., 2012).

In *Drosophila* photoreceptor epithelial cells, the apical complex aPKC/PAR-3/ PAR-6 is known to recruit PTEN to the developing cell-cell junctions (Pinal N. et al., 2006). CDC 42 was shown to be involved in the trafficking of proteins to the baso-lateral plasma

membrane in mammalian kidney epithelial cells. In another example of Madin-Darby Canine Kidney (MDCK) cell, as the culture grow to confluence, initial asymmetry at the membrane and hence cell polarization, is known to be provided by Cadherin-mediated cell-cell contact. This cue, in turn, recruits the Sec6/8 complex, which permits the sorting of proteins to the baso-lateral domain (Thomas and Williams, 1999). In another instance, the asymmetric division of neuroblasts (neuronal stem cell) giving rise to daughter cells, was also found to be remarkably aided by the presence of polarized localization of a number of proteins on the apico-basal axis (Wodarz, 2005).

When does this epithelial like polarity establishment take place?

Phenotypic analysis of the polarity proteins in *C. elegans* and *D. melanogaster* indicate that the event of PM polarity inception operates only within a very narrow time window that follows the actual initiation of apico-basal polarity during earlier developmental stages. In *C.elegans*, this initiation of PM polarity has been very well characterized. In the beginning, the *C.elegans* oocyte shows no developmental polarity in prophase I of meiosis. But after fertilization and completion of meiosis, the oocyte nucleus and the sperm donated centrosome gets differentially localized to the presumptive anterior and posterior ends of the cell of the cell respectively. This crucial time window for establishment of polarity in a single cell arises mainly due to the contractile forces generated by the actomyosin network. As a consequence of this, the PAR proteins and aPKC achieves their asymmetric distribution inside the cell.

In *Drosophila*, early embryonic development is syncytial (nuclear division without cytokinesis) and the blastoderm epithelium forms de novo through a process known as cellularization. Following fertilization, the first nine divisions generate a cloud of nuclei, most of which

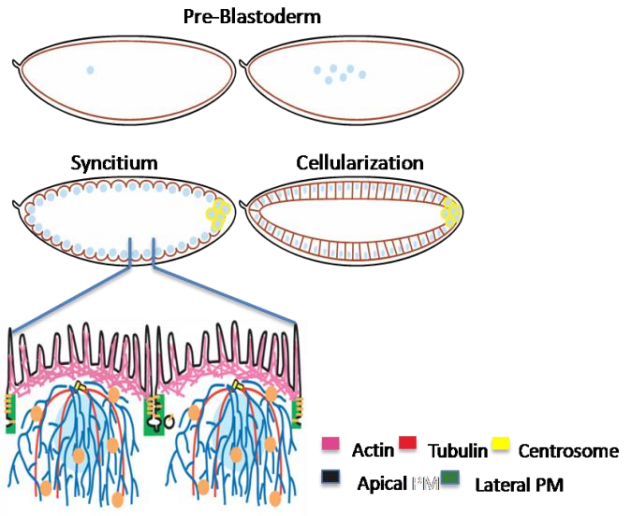

Fig.1.2. Schematic showing the early developmental stages namely, pre-blastoderm (till NC 10), syncytium (NC 10-13) and cellularization (NC14) of Drosophila embryogenesis (Sherlekar, Rikhy, 2011).

migrate from the middle of the egg toward the surface, where they form a monolayer called the syncytial blastoderm. The early nuclear divisions are synchronous and extremely rapid, occurring about every 8 minutes After another four rounds of nuclear division, plasma membranes (furrow canals) grow inward from the egg surface to enclose each nucleus, thereby converting the syncytial blastoderm into consisting of about 6000 separate cells. During cellularization, the furrow canals expand as a result of polarized insertion of newly synthesized plasma membrane and adjacent cells begin to form polarized cell–cell contacts (Lecuit T.et al., 2000) (Figure 1.2). Hence, some aspects of apico-basal polarity are in effect present even before the completion of cellularization.

Syncytium as a model system to study inception of Plasma Membrane Polarity

Digging more into the aspect of exact time window of PM polarity initiation, syncytium (Figure 1.3A) turned out to be a very important stage. Briefly, syncytium, as already mentioned, consists of 4 nuclear division cycles (NC 10-13). Each cycle consists of interphase, prophase, anaphase, telophase (Figure 1.3B). During metaphase of each cycle, the membrane (metaphase furrows) ingresses the most and later on it regresses back, only to ingress to even greater extent during metaphase of the next NC.

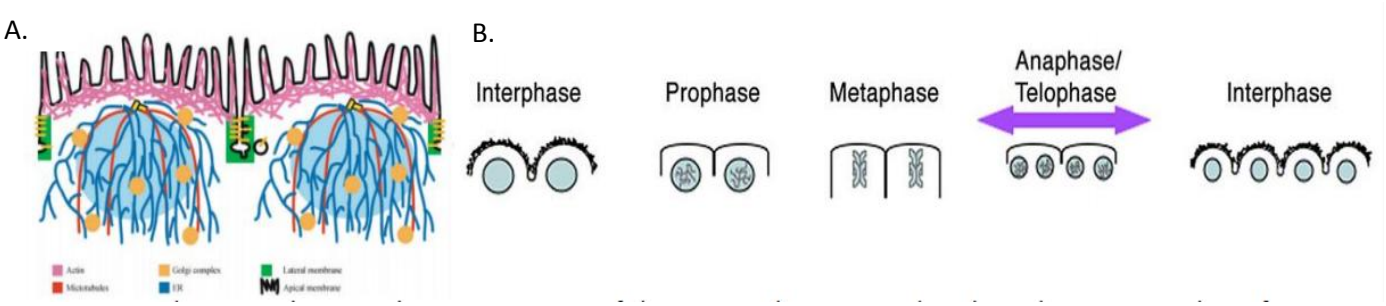

Fig.1.3. (A) Schematic showing the organization of the syncytial PM around each nucleus in interphase from NC 10 onward (Sherlekar and Rikhy 2011). (B). Remodeling of the PM in the syncytial embryo during each NC (Sokac and Wieschaus, 2008).

Recent insight into syncytial division cycles revealed that PM polarity, in terms of lipid and protein based asymmetry, is maintained even at this early stage (Mavrakis and Rikhy, 2010). Upon nuclear arrival at the cortex, the endoplasmic reticulum (ER) and Golgi were found to segregate among nuclei, delivering secretory products to the PM in

a spatially restricted manner (Frescas et al., 2006). Phospholipids like PIP3 and proteins like Growth associated protein 43 (Gap43) were found along the entire PM in syncytium, while DPatJ was found only at basal regions. DE-Cadherin (an adherens junctional protein) and Toll (a trans-membrane protein) were present in PM between adjacent nuclei and not in the microvillus PM region over nuclei. Further, diffusion studies on the PM also show that the PM is not freely shared between nuclei either (Mavrakis and Rikhy,2010). This phenomenon is remarkable in that there is no complete cell in the system despite which compartmentalized 'pseudo epithelial cell-like' characteristics are seen, hinting at the formation of some barriers in the PM which could be resulting in the compartmentalization. Barriers in the PM can be thought of to form with the formation of junctions between adjacent PM. If there are primitive junctions like AJs or their components thereof, it points towards the presence of polarity molecules that might be directing their formation or vice versa. With all this idea to look how PM polarity initiates, the syncytial system acts a good model system in *Drosophila* to investigate upon. The rapidly dividing syncytial *Drosophila* embryo reforms a polarized plasma membrane at least 3 times in one hour and is likely to be a good model system to study the onset of plasma membrane organization and epithelial like packing during embryogenesis.

Preliminary results from the previous related lab work (Ramya Balaji, Aparna Sherlekar, Bipasha Dey and Richa Rikhy)

Characterization of distribution of proteins present in epithelial cells in the syncytial embryo revealed association of DE-Cadherin, Toll, and Bazooka with the plasma membrane from the syncytial NC 12 onwards. Sep2, Bazooka and PatJ were found to label the basal region of the membrane from this time too. Along the vertical axis of the lateral membrane, polarized protein distribution was shown to exist in at least three domains, one apical and two lateral as shown in Fig 1.5. Another interesting observation was the unique localization pattern of certain polarity proteins like bazooka being present mostly on edges of the "pseudo-epithelial cells" while phospholipids like tGPH being present all over.

It was also seen that as the nuclear density of the syncytium increases, the membrane caps around each nucleus are more close to each other, thus efficiently packing of the membrane with every NC (as shown in Figure 1.4). The lateral membrane ingression in metaphase was noted to acquire a polygonal shape only from NC 12 onward and by metaphase of NC 13 shapes become very prominent. And in NC 12 itself, there exists a balance mostly between pentagons, hexagons and heptagons with hexagons being the most frequent ones which is continued till cellularization (as shown in Graph 1.1).

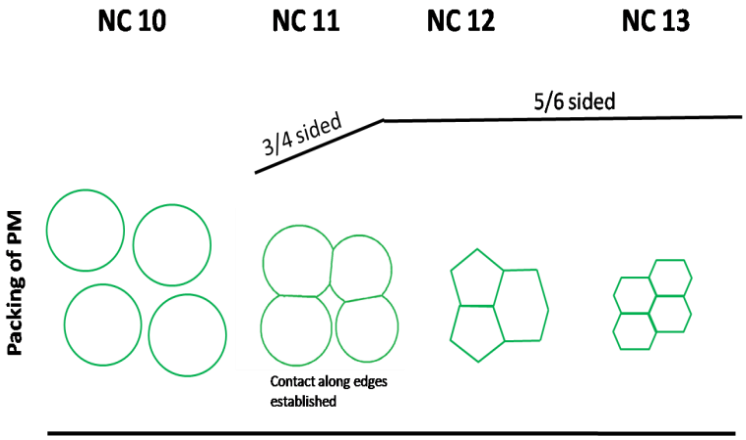

Fig.1.4. Schematic showing the packing of polygonal epithelial cells across NC 10 – NC 13. (By: Ramya Balaji.)

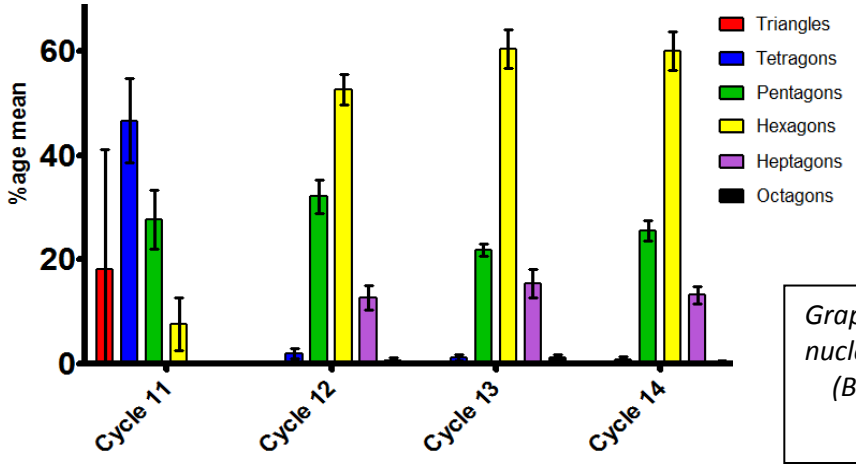

Graph.1.1. Polygonal distribution across nuclear cycles (NCs) 11-14. (By: Aparna Sherleker and Bipasha Dey.)

Proteins present in different domains along the lateral membrane

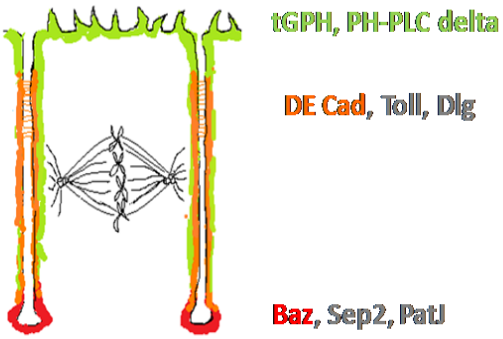

Fig.1.5. Schematic showing polarized protein distribution across one apical and two lateral domains in the lateral membrane during syncytium. (By: Ramya Balaji.)

Motivation of the project

Following up with the above study, the need to characterize the PM architecture in more detail, finding out the temporal onset of the association of the above proteins with the membrane, and gaining deeper insights into the mechanistic aspect of PM polarity initiation during syncytial division cycles cannot be overlooked. It calls for observing the plasma membrane organization in different dimensions (both X-Y axis and X-Z axis of the lateral membrane domain) as well as analyze the features of the PM when certain key proteins during PM polarity initiation are depleted in this particular time window of development. Some of the related questions embarked upon are:- What is the distribution pattern of the cytoskeletal and junctional proteins during syncytium? When does this unique pattern come up during embryogenesis? What kind of dynamic behavior/mobility do these proteins show? What would happen if these proteins are depleted during syncytium?

Objectives

1. Analysis of organization of polarized proteins in plasma membrane architecture.
2. Characterizing the dynamics of these proteins with the help of diffusion studies using photo bleaching experiments.
3. Deriving a mechanism for the polarized organization of the plasma membrane through disruption of cytoskeletal and junctional proteins.

Materials

All fly lines are obtained from Bloomington Stock Center, Indiana and grown up under standard conditions at 25ºC unless otherwise mentioned.

CS (+/+) - Wild type flies for Control Experiments (Krishanu Dey)
Wimp/+- One chromosomal copy of wimp with a wild type copy used as control in wimp mutant flies.

Transgenic Fly Lines Used:

1. Ubi-DE-Cadherin GFP - Ubiquitin promoter driven DE-Cad GFP line.
2. tGPH - GFP tagged PH domain construct that labels PIP3.
3. UASp-Toll Venus (Manos Mavrakis)
4. UAS Baz-GFP
5. UAS Sep2 GFP (Andrew Wilde)
6. UAS Peanut mCherry (Manos Mavrakis)
7. Nanos gal4

Fly lines used for depleting specific proteins:

1. *Wimp* Sb/ TM3, Ser
2. shg^{6115}/ Cyo.
3. baz^{19A} / Fm7c.

Targeted expression of genes driven by Gal4

Gal4/UAS system is used for directed gene expression in *Drosophila* (Brand and Perrimon, 1993). Briefly Gal4 is a yeast transcription factor that was shown to activate transcription in *Drosophila* (Fischer et.al, 1988). In this work, Nanos Gal4 (highly expressed during oogenesis) is crossed to the fluorescently tagged fly lines of Bazooka, Sep2, Peanut and Toll which has the Gal4 binding site (the UAS i.e. Upstream Activation Sequence) within its promoter. The idea is to transcribe the gene of interest only in those cells and tissues where Gal4 is expressed.

Wimp Strategy for targeted protein depletion

Wimp is a dominant maternal effect change-of-function mutation, allelic to a RNA Polymerase II subunit (RpII140) which causes reduced transcription of its interacting gene (Alerting, 1991). Maternally reduced shg^{6115} and baz^{19A} embryos were obtained using this wimp mutation. Due to specific interactions between the transcription factors and RNA Polymerase, protein levels of these targeted genes is considerably reduced in the flies with both shg^{6115} / baz^{19A} and the *wimp* as compared to *wimp* control flies.

Antibodies

Primary Antibodies - Amphiphysin, Bazooka, Phalloidin, Anti GFP, Anti-Peanut.

Secondary Antibodies - Alexa Fluor 488, 568, 633 conjugated goat anti-mouse, anti-rabbit (1:1000) from Invitrogen, DAPI / Hoechst to stain DNA (405 nm).

Slowfade Gold Antifade Reagent (Invitrogen) for mounting of fixed embryos onto the slides.

Methods / Procedures

Egg Collection - Flies obtained from the cross both at 25°C and 29°C were kept in cages. Embryos were collected on yeasted agar plates for 2.5-3 hours at the respective temperatures.

Lethality testing - After washing the embryos with distilled water and collected on a sieve, they were arranged in a matrix form on agar plate and kept at 25°C and 29°C. After every 24 hours and 48 hours of watch, number of lethal embryos was counted.

Immuno-staining – After egg collection, they were dechorionated in bleach, fixed for 15 minutes in 4% paraformaldehyde: heptane and devitellinized in heptane: methanol, and as well as hand divitellinized in PBST (PBS+ 0.3%Triton). The embryos were subsequently blocked with 2% BSA in PBST. Incubation primarily with primary antibodies at 4°C overnight, and subsequently with secondary antibodies were followed using standard protocol (Rothwell and Sullivan, 2007) Embryos were washed in PBST and mounted on slides with Slow Fade Gold Antifade Reagent from Invitrogen in preparation for microscopy.

Image Acquisition

1. **Imaging of fixed samples-** All confocal imaging of fixed embryos were done at room temperature (23°C) using an LSM-710 or 780 inverted microscope (Carl Zeiss, Inc. and IISER Pune microscopy facility) with excitation at 488 nm or 543 nm, and emission collection with PMT filters. A Plan Apochromat 40x/ 1.3 NA (for LSM 710) and 1.4 NA (for LSM 780) oil objective, with pinhole of 90.03, averaging of 4, acquisition speed of 7, zoom of 3 was used for imaging with the help of Zen software.
2. **Live Imaging -** Flies were kept in a cage at 25ºC. After 1.5 – 2 hour embryo collections on a yeast agar plate, they were washed in water, dechorionated in bleach and placed dorso- or ventro-laterally in coverslip chambers (LabTek). After covering the laid embryos with 2 ml of 1X PBS, imaging was done with above mentioned microscopes with averaging of 2, scan speed of 10 and zoom of 3. Z-stacks were taken from the apical surface of the embryos touching the coverslip to

approximately 15 -18 slices inside the embryo (length of each Z-stack was 1.08µm). During imaging of DE-Cadherin GFP, a highly sensitive (40% more sensitive than the PMTs) detector called GaAsP detector was used for better acquisition.

3. **Photo bleaching experiments-** Venus and GFP photo bleaching experiments were performed on a Zeiss LSM 780 laser scanning confocal microscope by photo bleaching a region of interest (ROI) and monitoring fluorescence recovery or loss over time as referred in (Mavrakis *et al.*, 2008). Images were acquired at optical zoom 4.0, argon laser power of 2%. 38 iterations at 100% transmission were used for photo bleaching at a single plane. Three pre-bleach images were acquired in both FRAP and FLIP protocols. Images were typically acquired every 1 millisecond until the extent of ROI signal recovery after photo bleaching is stabilized. In both these photo bleaching experiments, one edge of an epithelial cell is bleached with a fixed area of 1.71µm^2 while the neighboring, non-neighboring, and reference (one away from the bleached cell) edges are used for monitoring from where the pool of recovery comes as indicated in Fig.2.1. This process is repeated from NC 12 in syncytium till cellularization.

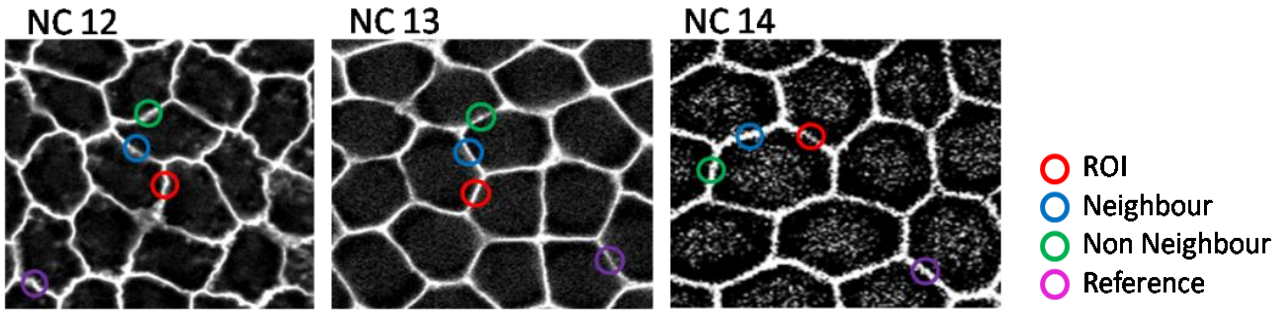

Fig.2.1. PM labeled with a phosphoplipid across nuclear division cycles 12 to 14 indicated by circular regions marked with different colors and are used for monitoring of intensity during photo bleaching .

Image Analysis

Description of measurements for studying plasma membrane organization during both syncytium and cellularization

1. **Frequency distribution of polygonal packing –** For representing the polygonal packing in terms of polygonal classes, they have been visually marked for the number of edges (and hence which polygonal shape) in each compartment using the Z-section with most compact metaphase packing (Fig.3.18A). The analysis was done for at least 3 time-lapse data sets.
2. **Description of intensity analysis (X-Y plane) -** It represents the distribution of the membrane intensities across edges and vertices through each nuclear division cycle of each type of PM labeled fluorescently tagged fly line. Intensity measurements in each movie comprised firstly of identifying metaphase of each syncytial nuclear division cycle (NC 10-13) and cellularization. At this phase, the X-Y plane with maximum intensity of fluorescent membrane signal was chosen for further analysis in accordance with the intensity measurement done along the z stacks during every NC of the respective proteins (Master's thesis by Ramya Balaji). The regions of interest (edges and vertices of the lateral membrane) were drawn using the "segmented line" tool as indicated in the figure below. Mean gray values with the corresponding ROIs were measured using the "ROI Manager" plugin in ImageJ. The intensity values are in arbitrary units and are not scaled to be compared across graphs for each of the membrane labels. And the sample size of entire analysis is reported as N = total no. of edges and vertices (ROIs) measured for each NC in a single embryo, total number of embryos. For e.g., in NC 13, 30 edges and 30 vertices = 10 edge X 3 embryos and 10 vertices X 3 embryos). The mean intensity value per unit area obtained from the software for each NC in a single embryo was normalized with respect to the total intensity of the entire scan field after subtracting both the values from the background intensity value. This calculation is averaged for each NC for three embryos. Standard error of mean (SEM) have also been indicated in the column graph. Two-tailed unpaired student's T-test was performed to compare

between edges and vertices of each NC. Significant values $p<0.05$, $p<0.01$, $p<0.001$ have been denoted by in the graph by *, **, *** respectively.

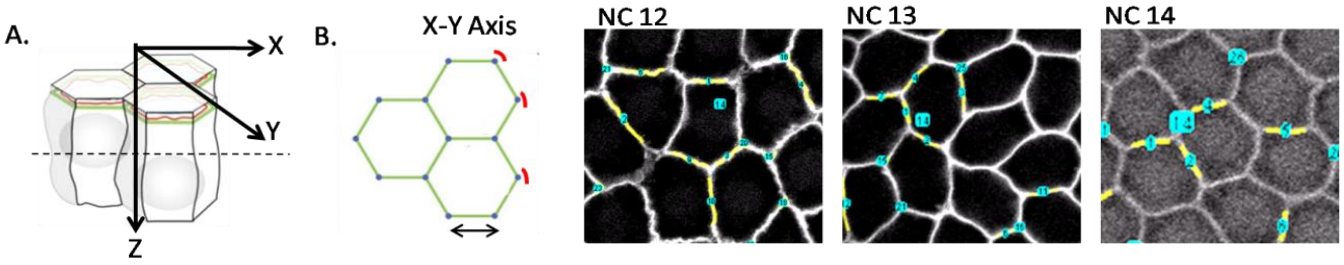

Fig.2.2. (A) Schematic of the X-Y plane chosen to measure intensity of the lateral membrane in the epithelial cells. (B) Cross section of the lateral membrane through the dotted line in (A). In the X-Y plane the edges are indicated with black arrows and vertices with red curved lines. (C) Representative Z-sections for measurement of intensity in different nuclear division cycles. The yellow line drawn over the edges and vertices indicate the ROIs.

3. **Fluorescence Recovery after Photo bleaching (FRAP) Analysis -** Raw fluorescence intensity measurements were background subtracted, corrected for the bleached fraction (for FRAP), laser fluctuations and photo bleaching during acquisition, and finally normalized to arbitrary fluorescence units (pre-bleach time points normalized to one) as described in (Rabut and Ellenberg, 2005). Fluorescence recovery curves were plotted using Microsoft Office Excel 2000 and Graph Pad Prism 5.
4. **Fluorescence Loss in Photo bleaching (FLIP) Analysis–** Raw fluorescence intensity measurements were background subtracted and corrected by dividing the fluorescence measurement at each time point by a function representing the temporal artifactual signal variation from an unbleached cell within the scan field. Then the values were normalized to an arbitrary fluorescence unit and were plotted as mentioned in the FRAP analysis above.

Results

We have chosen several fluorescently tagged transgenic fly lines of both ubiquitous over-expression as well as gal4 driven over-expression to give us detailed insight of broadly three basic aspects of epithelial cells during development - its initiation of polarity, membrane architecture and tissue packing. The proteins targeted for this are categorized functionally as mentioned in the Table 3.1.

Functional class	Fluorescent labels	Antibodies
Junctional Polarity	Bazooka GFP, DE-Cadherin GFP	Anti-Bazooka, Anti-GFP
Cytoskeletal Remodeling Protein	Peanut mCherry, Sep2 GFP	Anti-Peanut
Lipid binding	tGPH GFP	

Table 3.1. List of all the proteins categorized based on their function used to study onset of PM organization in the Drosophila embryo.

Each of these chosen proteins is known to have a polarized organization already on the plasma membrane of epithelial cells.

tGPH, GFP tagged PH domain of GRP, a PIP3 (phosphatidyl-inositide phosphate 3) marker that labels the entire plasma membrane and demonstrates the polygonal architecture of epithelial cells (Britton et al., 2002).

DE-Cadherin is a protein component of Adherens Junction (AJ) located sub-apically in the lateral domain of the PM of epithelial cells. It is known to interact with adjoining cells via homophillic interactions with other Cadherin molecules (Harris and Peifer, 2004).

Peanut and Sep2 are the proteins belonging to the Septin family, localized basally with respect to the junctional protein, in the furrow canal of ingressing plasma membrane during syncytium. They play an important role in organization of actomyosin during membrane constriction due to the bundling and curving activity of Septins on actin filaments (Founounou et al., 2013) .

Bazooka is a membrane associating polarity protein, which, in mutual dependence with aPKC, is responsible for formation and maintenance for epithelial apico/basal polarity. It is localized asymmetrically in the baso-lateral domain of the PM during syncytium and gets transported sub-apically in cellularization (Wodarz et al., 2003).

I. Analysis of Localization Pattern of Polarity and Cytoskeletal Remodeling Proteins on Plasma Membrane in the Syncytial Fly Embryo

Time lapse confocal laser scanning microscopy of fluorescently tagged tGPH, DE-Cadherin, Bazooka, Sep2 and Peanut in four dimensions has demonstrated differential localization pattern of proteins across edges and vertices along the X-Y axis in the lateral domain of the PM during *Drosophila* embryogenesis. The stage chosen for depiction is late prophase or metaphase when the lateral domain is the longest.

Ia. Differential distribution of proteins in the XY plane of the *Drosophila* embryo

Differences in distribution of proteins in the PM are observed mainly in tGPH, Bazooka and Peanut. tGPH labels the complete plasma membrane and shows a polygonal distribution. It labels the edge and vertex of each polygon uniformly whereas Bazooka labels edges more brightly as compared to vertices and Peanut from the Septin family labels vertices more brightly as compared to edges (Fig.3.1).

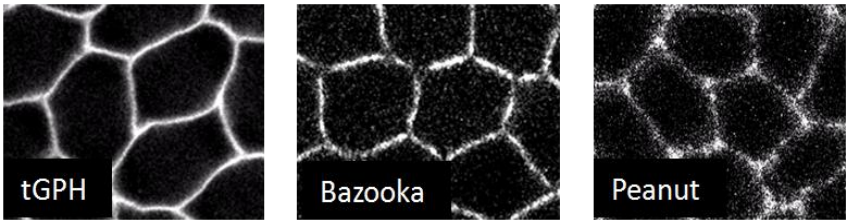

Fig.3.1. ***Representative sections of polarized PM in X-Y plane****. tGPH is present uniformly over edges and vertices. Bazooka mostly absent in vertices while Peanut present mainly in vertices.*

The observation that certain proteins like Bazooka and Peanut getting asymmetrically distributed across edges (Bazooka) and vertices (Peanut) of the syncytial pseudo epithelial cell, then prompted us to carefully study the association of these proteins with the PM over time. The following series of figures show fluorescent intensity distribution along X-Y axis over every nuclear division cycle in syncytium and cellularization.

I b. Temporal analysis of tGPH distribution in the syncytial plasma membrane

PM labeled with tGPH demonstrate the polygonal architecture of the epithelial cells in X-Y axis and is observed to be uniformly distributed across edges and vertices from NC 12 till NC 14 (Graph.3.1.B).

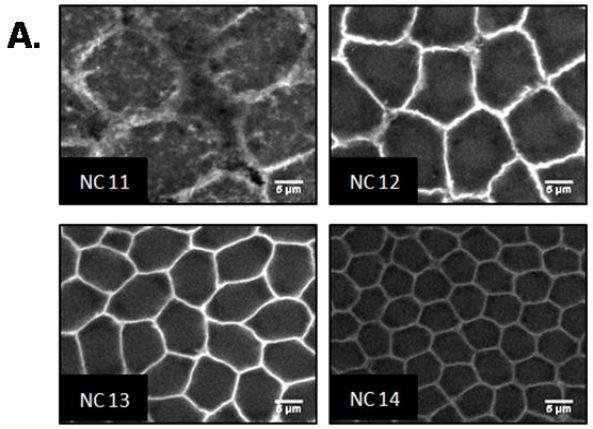

Fig.3.2 (A). *Panel showing lateral membrane labeled with tGPH GFP across NC 11-NC 14.*

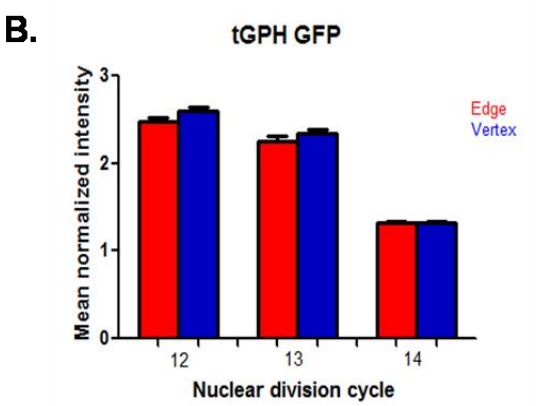

Graph.3.1 (B). Mean normalized intensity across edges and vertices of the PM labeled with tGPH GFP from NC 11-14. (N=3, 30).

I c. Temporal analysis of Cadherin distribution in the syncytial plasma membrane

DE Cadherin, seems to start associating with the lateral domain of the PM from NC 12 onwards. At this stage, the edge intensity is less than that of vertex. In the next cycle however, this trend is reversed. Edges have more accumulation of GFP tagged Cadherin molecules than vertices. This symmetric distribution is continued over time during cellularization when a complete epithelial cell is formed (Graph.3.2 (D)).

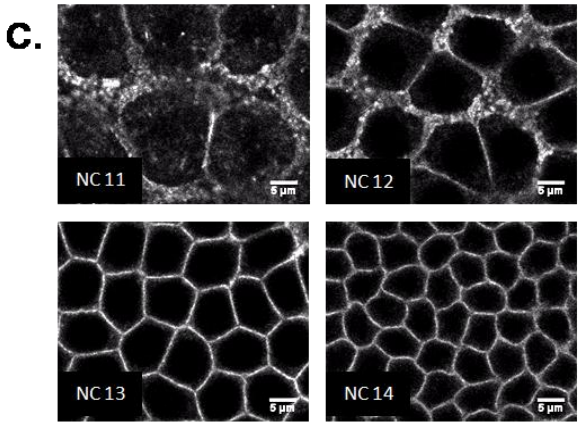

Fig.3.3 (C). Lateral membrane labeled with DE-Cadherin GFP across NC 11- 14.

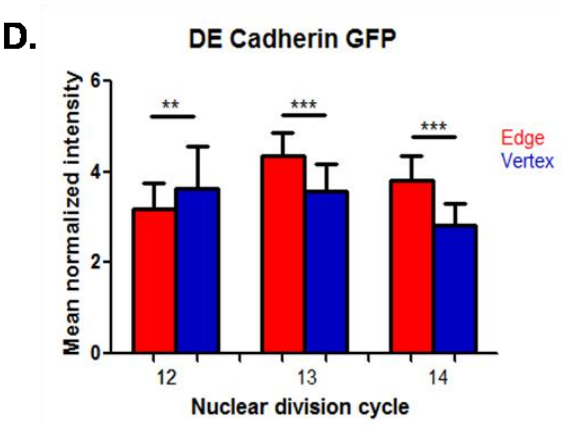

*Graph.3.2 (D). Mean normalized intensity across edges and vertices of the PM labeled with DE Cadherin GFP from NC 11-14. p<0.01=**, p<0.001=***. N=3,30.*

I.d. Temporal analysis of Bazooka distribution in the syncytial plasma membrane

GFP tagged Bazooka shows enriched protein accumulation on the edges as compared to the vertices from NC 12 onwards. As nuclear division cycle progresses, its distribution in the lateral membrane becomes more fragmented and look like punctae. This morphological feature is very prominently visible during cellularization although vertices continue to lack Bazooka throughout (Graph.3.3 (F)).

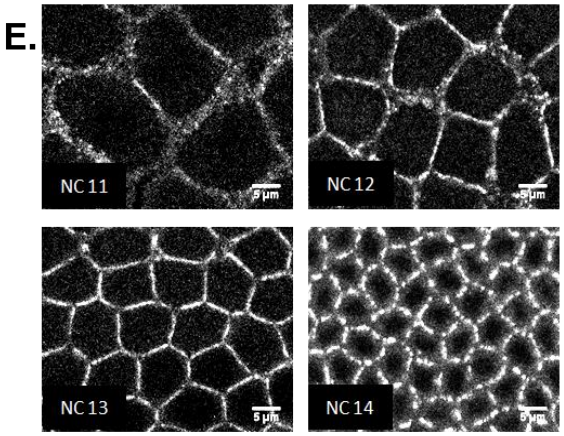

Fig.3.4 (E). Lateral membrane labeled with Bazooka GFP across NC 11-NC 14.

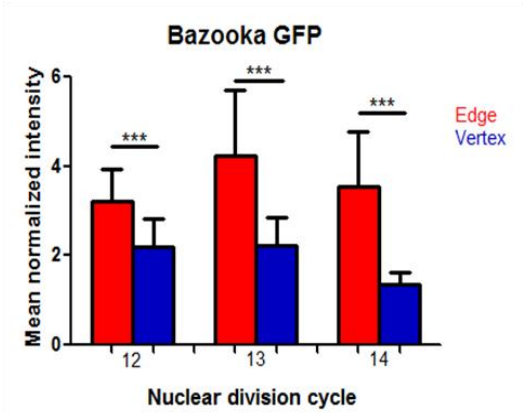

*Graph.3.3 (F).Mean normalized intensity across edges and vertices of the PM labeled with Bazooka GFP from NC 11-14. p<0.001=***. N=3, 30.*

This over-expressed GFP tagged Bazooka fly embryos, when co stained with both Anti-Bazooka and Anti GFP antibody, showed co-localization, with more intensity on edge and less on vertex during syncytial NC 12 and NC 13 (Graph.3.5.J). It also corroborated the distribution of endogenous Bazooka as observed in Anti-Bazooka staining of wild type embryos during NC 13 and NC 14 (Graph.3.4H).

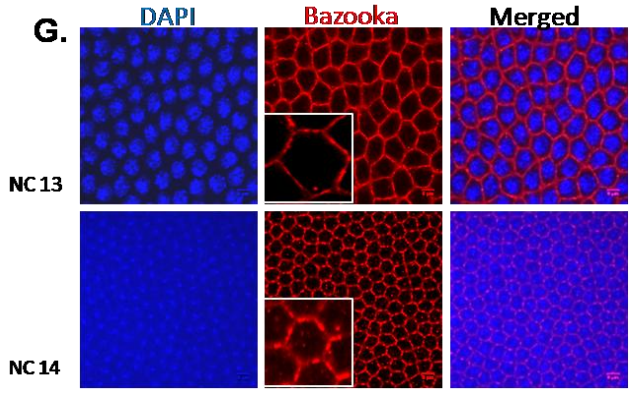

Fig.3.5 (G). Panel for Anti-Bazooka stained in wild type embryos showing distribution across edges and vertices from NC13-14.

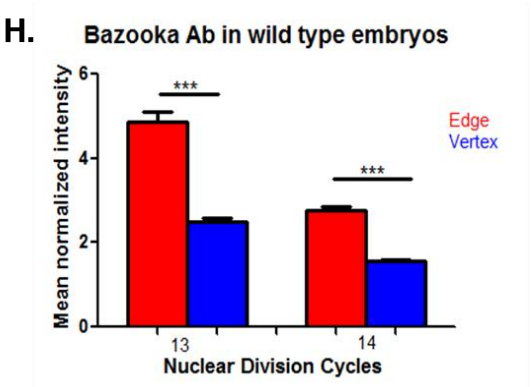

*Graph.3.4 (H).Mean normalized intensity across edges and vertices of the PM labeled with Anti-Bazooka in wild type embryos from NC 13-14. p<0.001=***. N=3, 30.*

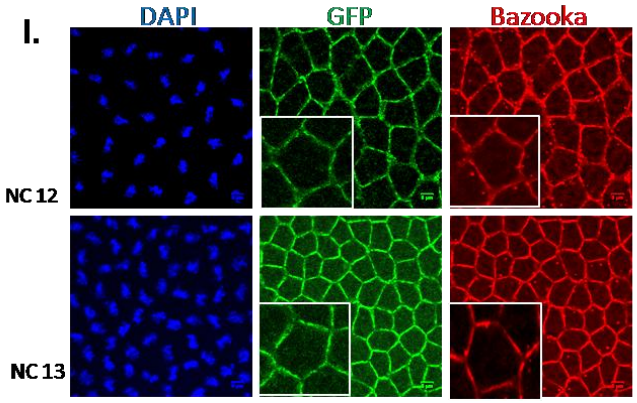

Fig.3.6 (I). Panel for Anti-Bazooka and Anti GFP stained in Gal4 driven Bazooka GFP embryos showing distribution across edges and vertices from NC12-13.

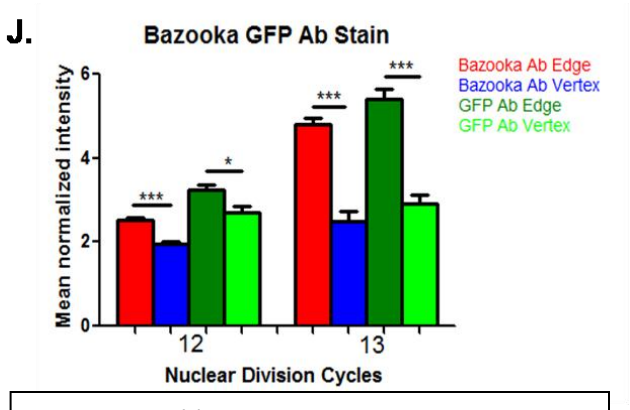

Graph.3.5 (J). Mean normalized intensity across edges and vertices of the PM labeled with Anti-Bazooka and Anti-GFP in Gal4 driven Bazooka GFP embryos from NC 12-13. p<0.05=, p<0.01=**, p<0.001=***. N=3, 30.*

I.e. Temporal analysis of the Septin family of protein distribution in the syncytial plasma membrane

In contrast to the distribution pattern of Bazooka GFP, the intensity of Sep2 in X-Y axis is significantly more on the vertices than on the edges. This differential localization pattern is found NC12 onwards (Graph.3.6.L). In cellularization, Sep2 has different localization pattern along the entire lateral membrane. At the tip of the ingressing furrow close to the contractile ring, it is broadly distributed in both edges and vertices. However in the sections above it, vertices show more intensity than edges (Fig. 3.7 K).

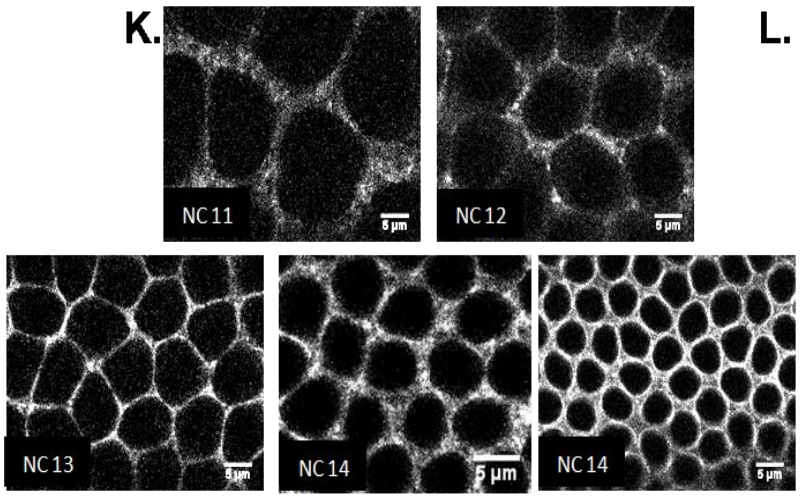

Lateral PM

Tip of furrow

Fig.3.7 (K). Panel showing distribution of Sep2 GFP across NC 12-14.

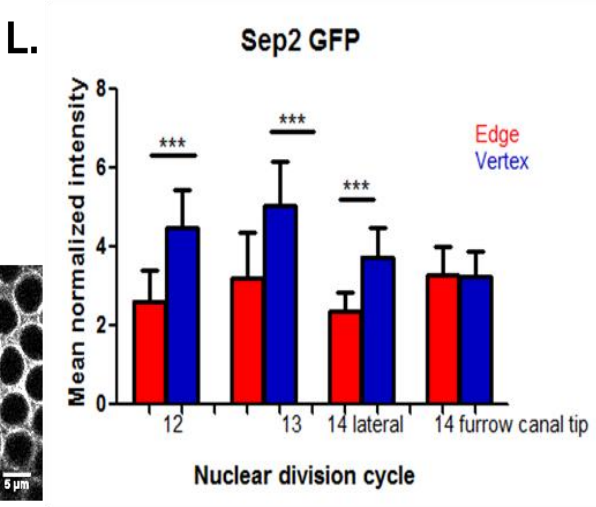

*Graph.3.6 (L). Mean normalized intensity across edges and vertices of the PM labeled with Bazooka GFP from NC 11-14. p<0.001=***. N=3, 30.*

Peanut shows similar distribution pattern of PM as Sep2 with its intensity being more on vertices as compared to the edges in the lateral membrane. This difference is discernible from NC 12 onwards (Graph.3.7.N). Corroborating the pattern of Peanut over-expression, the endogenous Peanut localization obtained by Anti Peanut immuno-staining in wild type embryos also shows more intensity in a vertex than an edge (Graph.3.8.P).

M.

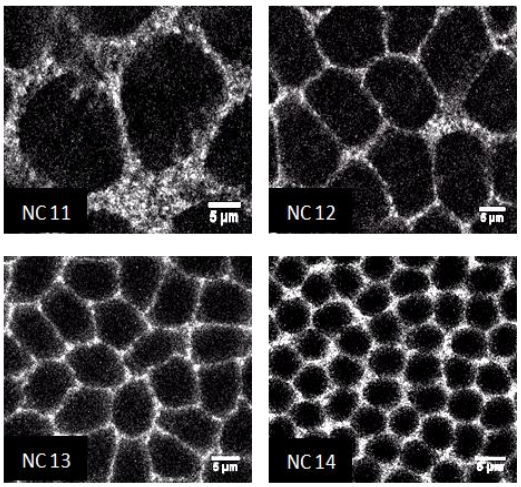

Fig.3.8 (M). Lateral membrane labeled with Peanut mCherry across NC 11-14.

N.

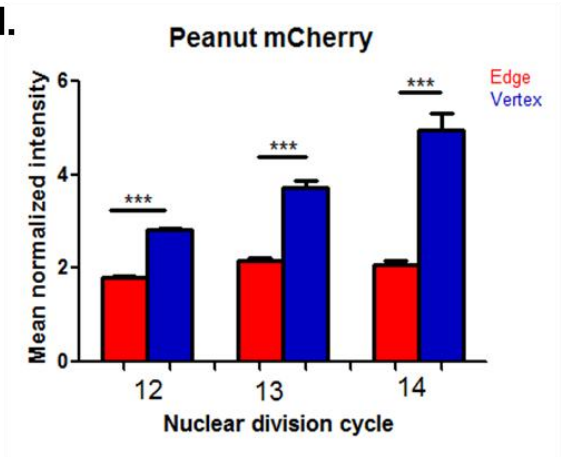

*Graph.3.7 (N). Mean normalized intensity across edges and vertices of the PM labeled with Peanut mCherry from NC 11-14. p<0.001=***. N=3, 30.*

O.

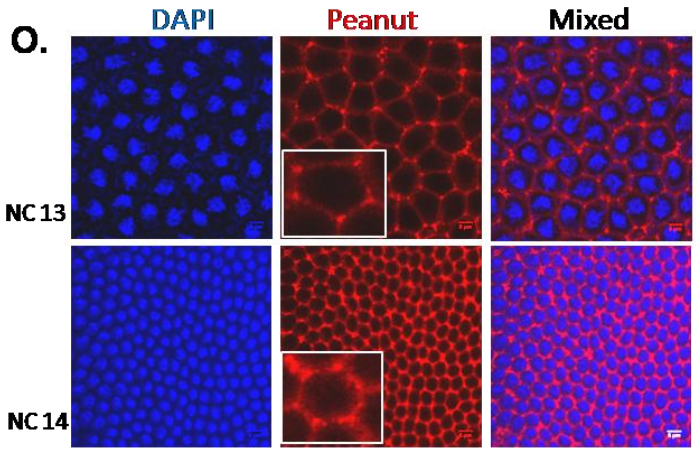

Fig.3.9 (O). Panel for Anti-Peanut stained in wild type embryos showing distribution across edges and vertices from NC13-14. Insets show magnified PM organization.

P.

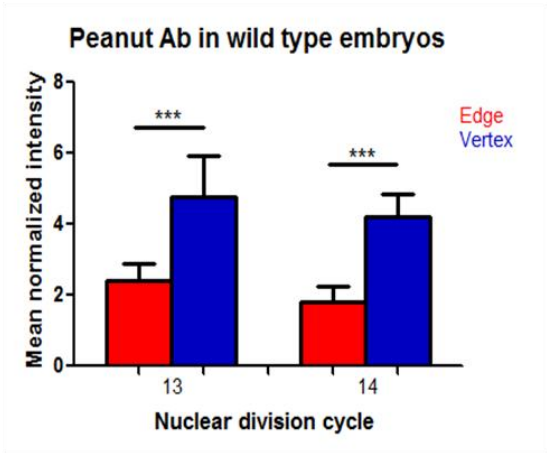

*Graph.3.8. (P). Mean normalized intensity across edges and vertices of the PM labeled with Anti-Peanut in wild type embryos from NC 11-14. p<0.001=***. N=3, 30.*

II. Understanding the dynamics of the cytoskeletal and polarity proteins with the help of diffusion studies (FRAP and FLIP).

Previous lab work shows partitioning of Bazooka out of vertices and Septins more in vertices in the metaphase lateral membrane of NC 12 and 13 indicating the presence of a barrier or inhibitory cue to their localization to the vertices/edges. Exactly what is different about the vertices compared to the edges except for more number of adjacent cap-to-cap contacts at vertices than just two adjacent cap contacts along an edge is still unclear. FRAP analysis at edges and vertices with the various fluorescently tagged PM markers could be one way to determine the presence or absence of diffusion barriers in the lateral membrane.

To follow this up, we studied the spatio-temporal dynamics of the proteins on the PM across edges via vertices during both syncytium and cellularization with the help of photo bleaching experiments, FRAP. A region of interest (ROI) on an edge is bleached and the intensity profile of the regions as indicated in Fig.2.1 is monitored over time. The proteins chosen for these diffusion studies are mainly based on different modes of their association with membrane and potentially different PM organization. To further find out what happens to the neighboring edges when the entire pool of protein of one particular edge is depleted, FLIP experiments were performed. In this, a particular ROI is bleached repeatedly over time until the intensity stabilizes to its minimum and intensity profile of all monitored regions is plotted during this time window.

II.a. Cadherin mobility in the plasma membrane

Photo bleaching a region of DE-Cadherin GFP at the pre-blastoderm stage (red circle, Fig.4.1.A), was followed by diffusion of fluorescent signal from outside the bleached box towards it, which resulted in the fluorescence recovery of the bleached ROI. (Graph.4.1.B). This phenomenon is shown by the intensity dip of the neighboring region beside the ROI (yellow circle, Fig.4.1.A) which indicates free movement of Cadherin molecules during this time window.

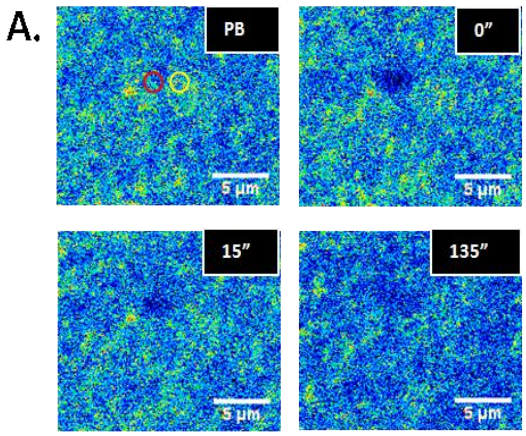

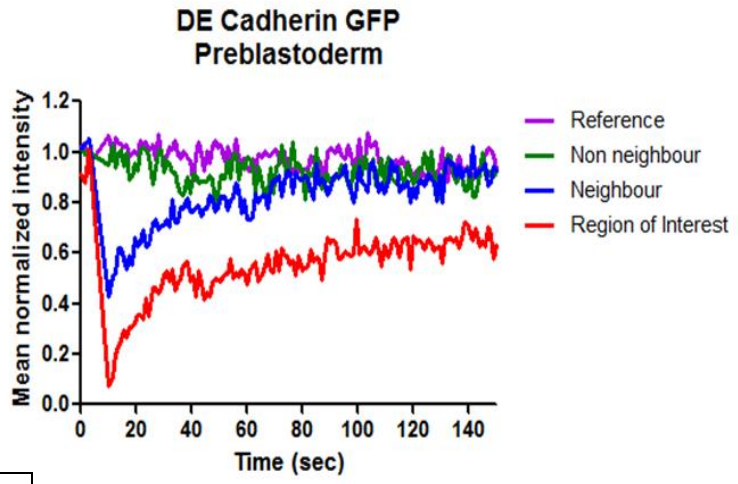

Fig.4.1 (A). Panel showing mobility of DE-Cadherin GFP during FRAP in pre-blastoderm at time points of pre-bleach (PB), bleach (0'), half recovery (15") and full recovery (135"). Red and yellow circles in PB indicate the ROI and the neighboring edge respectively.

Graph.4.1 (B). Temporal intensity distribution of DE- Cadherin GFP during FRAP in pre-blastoderm at the monitored regions. N=1 embryo.

During syncytium and cellularization, photo bleaching a ROI resulted in an intensity drop to 20%, from where the recovery was up to more than 80% within ~70-80 seconds. During this time, the neighboring (blue line) as well as non-neighboring edges (green line) did not show any corresponding decrease in intensity with the photo bleaching, indicating that there is no contribution of neighbor edge in the recovery of the bleached edge (Graph.4.1 D,F,H.).

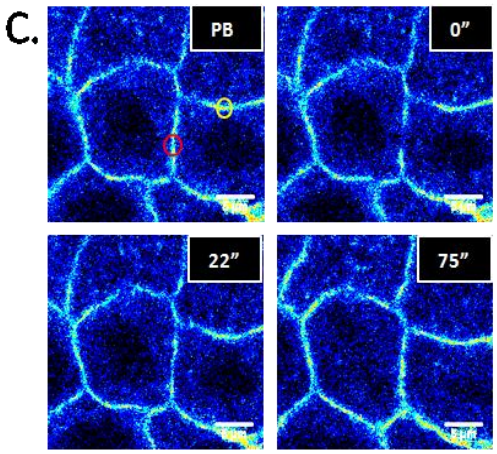

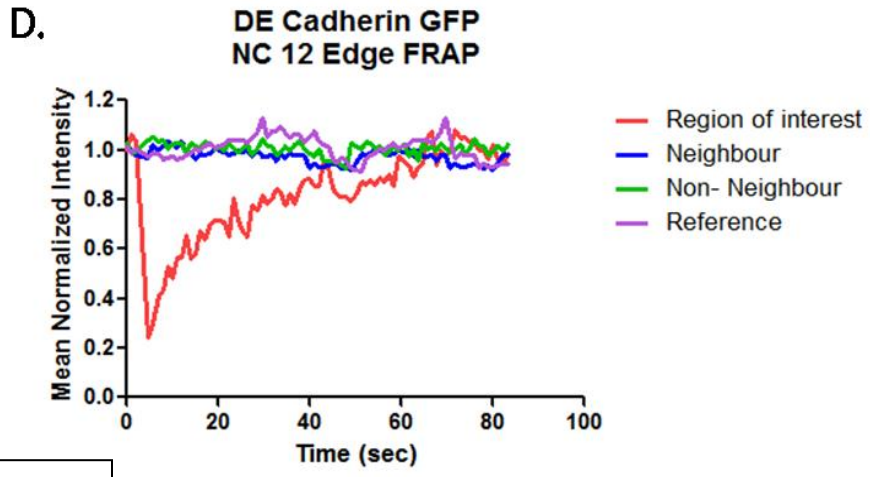

Fig. 4.1 (C). Panel showing temporal mobility of DE-Cadherin GFP during FRAP in NC 12 at time points of pre-bleach (PB), bleach (0'), half recovery (22") and full recovery (75"). Red and yellow regions in PB indicate the ROI and the neighboring edge respectively.

Graph.4.1 (D). Temporal intensity distribution of an edge in DE-Cadherin GFP during FRAP in NC 12 at the monitored regions. N=1 embryo.

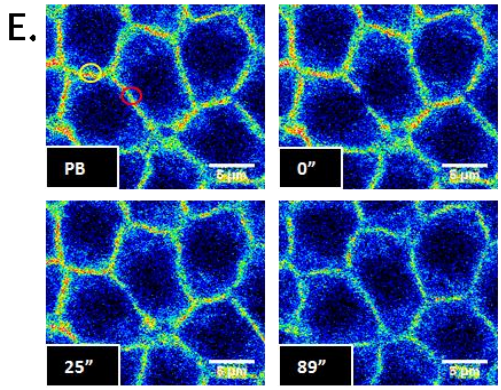

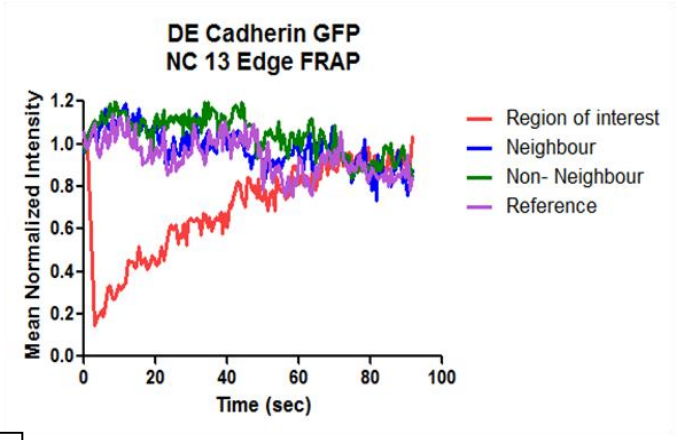

Fig.4.1 (E). Panel showing temporal mobility of DE-Cadherin GFP during FRAP in NC 13 in pre-bleach (PB), bleach (0’), half recovery (25”) and full recovery (89”). Red and yellow regions indicate the ROI and the neighboring edge respectively.

Graph.4.1 (F). Temporal intensity distribution of an edge in DE-Cadherin GFP during FRAP in NC 13 at the monitored regions. N=1 embryo.

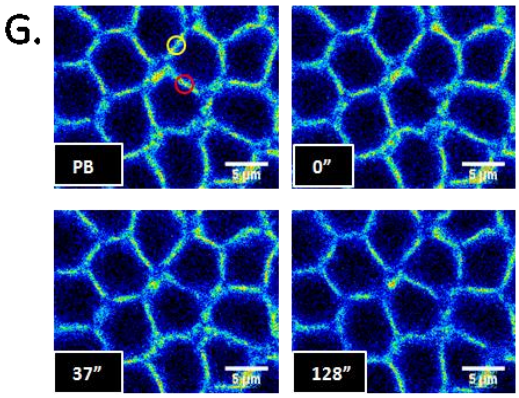

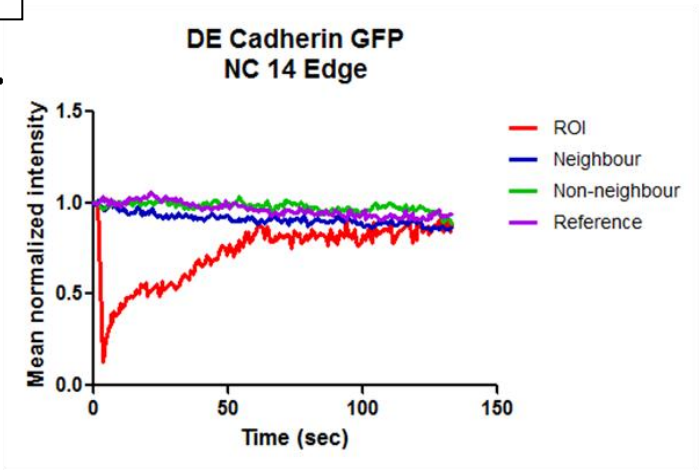

Fig.4.1 (G). Panel showing temporal mobility of DE-Cadherin GFP in pre-bleach (PB), bleach (0’), half recovery (37”) and full recovery (128”) during FRAP in cellularization. Red and yellow regions indicate the ROI and the neighboring edge respectively.

Graph.4.1 (H). Temporal intensity distribution of an edge in DE-Cadherin GFP during FRAP in NC 14 at the monitored regions. N=1 embryo.

During FLIP experiments in the syncytial cycles 12-13 and cellularization, continuous photo bleaching in the ROI led to a sharp drop in its intensity to ~ 5-10% within 20 seconds (Graphs.4.2.B, D, F). Neighbor region adjoining the bleached ROI (circle in light red, Fig.4.2 A, C, E) also showed a decreasing trend in the intensity over time due to free diffusion of Cadherin molecules within an edge. The fluorescence intensity in the

neighboring edges, on the other hand, was not found to be affected within this time period.

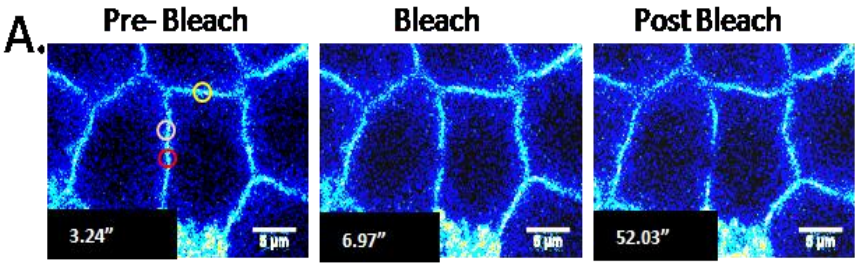

Fig.4.2 (A). Panel showing temporal mobility of DE-Cadherin GFP in pre-bleach (3.24"), bleach (6.97") and post bleach (52.03") images during FLIP in NC 12. Red and yellow regions indicate the ROI and the neighboring edge respectively. Circle in light red shows the neighbor region on the same edge as the ROI.

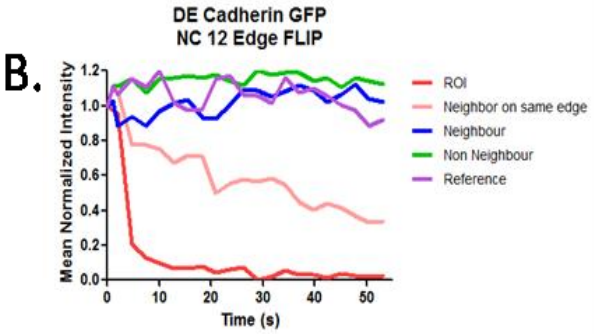

Graph.4.2 (B). Temporal intensity distribution of an edge during FLIP in NC 12 at the monitored regions. N=1 embryo.

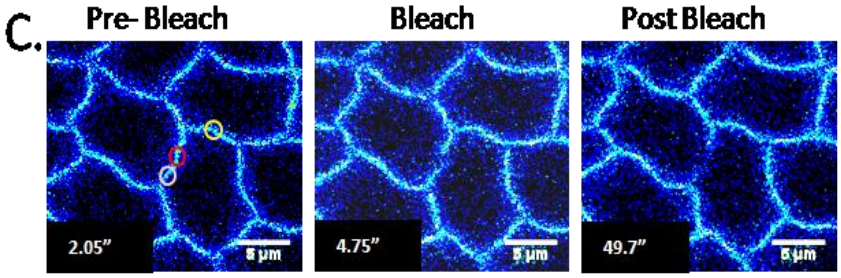

Fig.4.2 (C). Panel showing temporal mobility of DE-Cadherin GFP in pre-bleach (2.05"), bleach (4.75") and post bleach (49.7") images during FLIP in NC 13. Red and yellow regions indicate the ROI and the neighboring edge respectively. Circle in light red shows the neighbor region on the same edge as ROI.

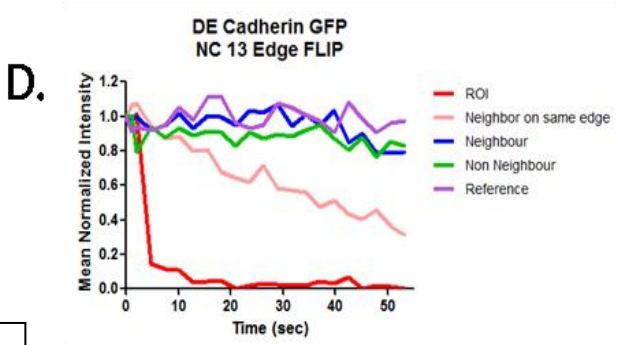

Graph.4.2 (D). Temporal intensity distribution of an edge during FLIP in NC 13 at the monitored regions. N=1 embryo.

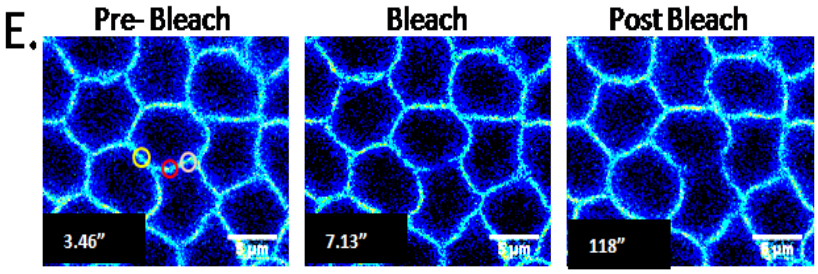

Fig.4.2(E). Panel showing temporal mobility of DE-Cadherin GFP in pre-bleach (3.46"), bleach (7.13") and post bleach (118") images during FLIP in NC 14. Red and yellow regions indicate the ROI and the neighboring edge respectively. Circle in light red shows the neighbor region on the same edge as ROI.

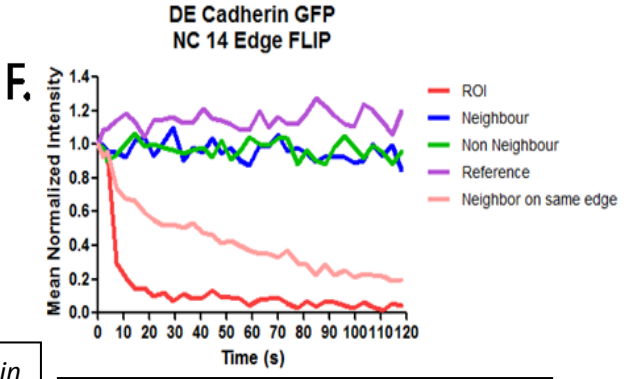

Graph.4.2 (F). Temporal intensity distribution of an edge during FLIP in NC 14 at the monitored regions. N=1 embryo.

To summarize, Cadherin shows compartmentalized diffusion of molecules within an edge of an epithelial cell from NC12-14.

II.b. Toll mobility in the plasma membrane

To understand more about the dynamic behavior of trans-membrane proteins during syncytium, we performed similar kinds of diffusion experiments with another protein Toll which is known to have similar functional and structural characteristics as Cadherin. Toll is a trans-membrane receptor protein which is involved in dorso-ventral patterning of the fly embryo. In mammalian *in vitro* cell culture studies, Toll is also demonstrated to be responsible for adhering of cells, presumably through interactions of its extracellular domains like Cadherin (Yuki. et al., 2013). Photo bleaching experiment on Toll was done to find out if the property of restricted mobility was unique to Cadherin only or is it a property of the entire class of trans-membrane proteins.

It was observed that in FRAP experiments, the extent of bleach during all the cycles of Toll Venus was less (from 100% to ~40%) as compared to DE-Cadherin GFP (from 100% to ~20%). The recovery of the fluorescent signal in bleached ROI was up to 90% within ~80-100 seconds in NC 12 (Graph.4.3.B). And this recovery was observed to be faster, i.e., within 60-70 seconds in the next syncytial cycle, NC 13 (Graph.4.3.D).

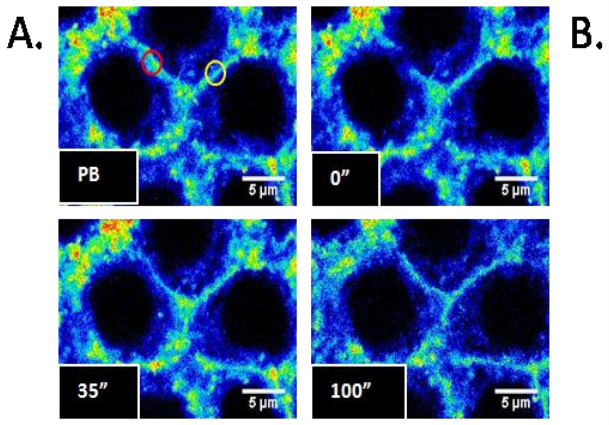

Fig.4.3 (A). Panel showing temporal mobility of Toll Venus in pre-bleach (PB), bleach (0'), half recovery (35") and full recovery (100") during FRAP in NC 12. Red and yellow regions indicate the ROI and the neighboring edge respectively.

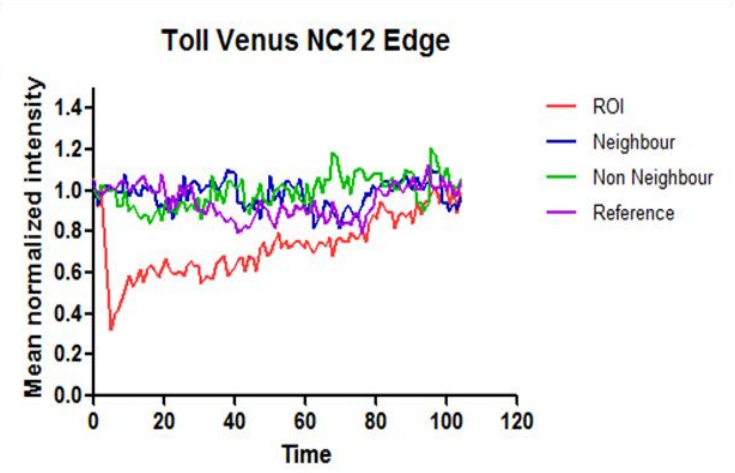

Graph. 4.3. (B). Temporal intensity distribution during FRAP in NC 12 at the monitored regions. N=1 embryo.

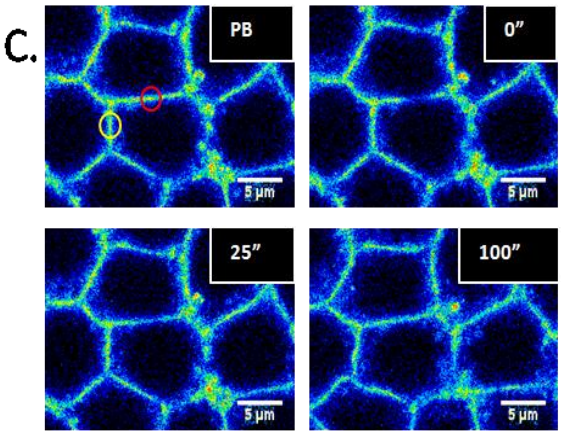

Fig.4.3 (C). Panel showing temporal mobility of Toll Venus in pre-bleach (PB), bleach (0'), half recovery (25") and full recovery (100") during FRAP in NC 13. Red and yellow regions indicate the ROI and the neighboring edge respectively.

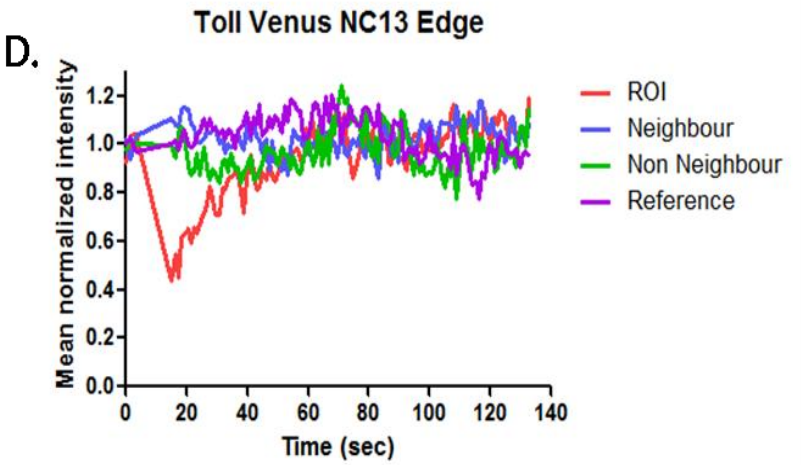

Graph.4.3.(D).Temporal intensity distribution on an edge during FRAP in NC 13 at the monitored regions. N=1 embryo.

And during cellularization, this time window of recovery gets shortened to only 30-40 seconds. To summarize, as opposed to the constant amount of time taken for Cadherin molecules to recover, Toll demonstrated a trend of decrease in time taken to do the same task. Nevertheless, the most interesting feature of neighboring edges not getting affected due to photo bleaching does not seem to change across both syncytium and cellularization.

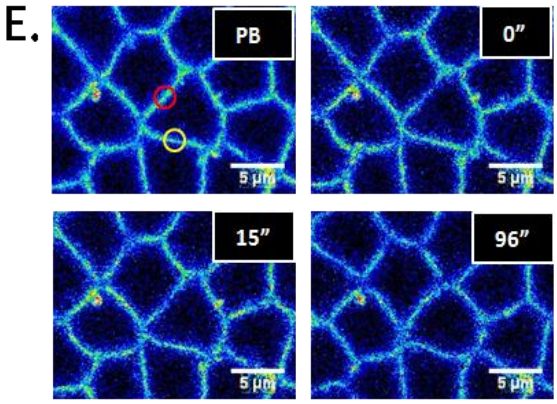

Fig.4.3 (E). Panel showing temporal mobility of Toll Venus in pre-bleach (PB), bleach (0'), half recovery (15") and full recovery (96") during FRAP in NC 14. Red and yellow regions indicate the ROI and the neighboring edge respectively.

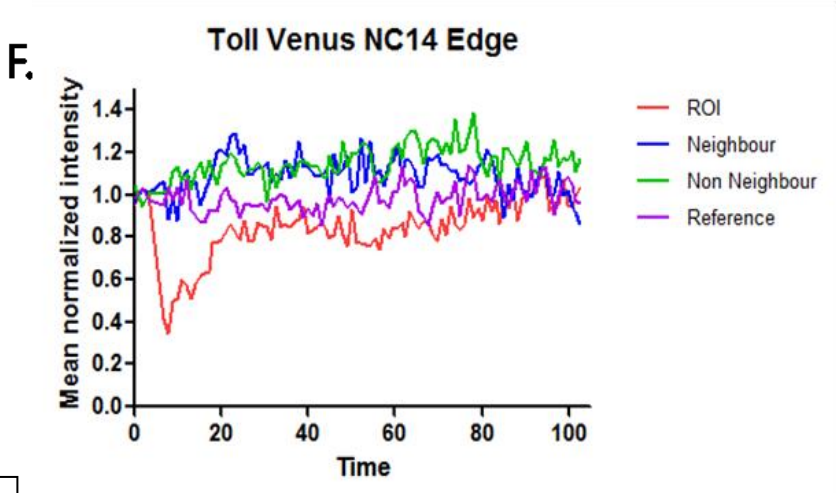

Graph.4.3 (F). Temporal intensity distribution on an edge during FRAP in NC 13 at the monitored regions. N=1 embryo.

Following a similar kind of trend as above in FRAP, repeated photo bleaching of Toll Venus in syncytial division cycles did not show any significant change in the intensity of the neighboring and non-neighboring edges. Only the neighboring area on the same edge showed a dip in the intensity profile over time indicating mobility of Toll restricted only within an edge (Graph.4.4.B, D).

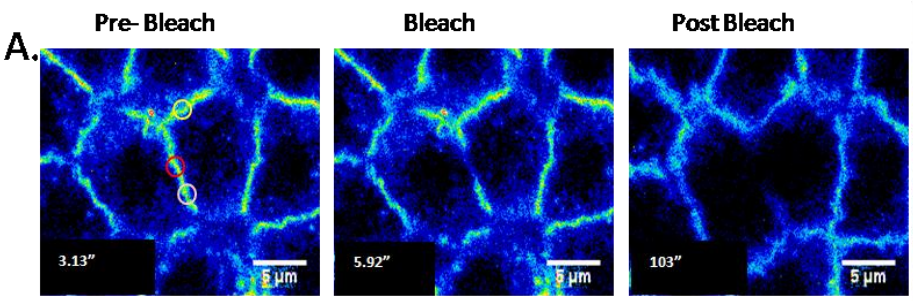

Fig.4.4 (A). Panel showing temporal mobility of Toll-Venus in pre-bleach (3.13"), bleach (5.92") and post bleach (103") images during FLIP in NC 12. Red and yellow regions indicate the ROI and the neighboring edge respectively. Circle in light red shows the neighbor region on the same edge as ROI. - (with Bipasha Dey).

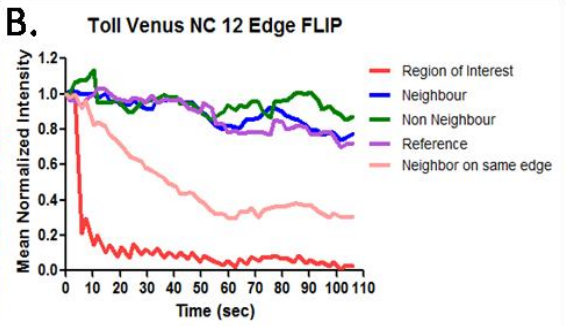

Graph. 4.4. (B). Temporal intensity distribution of an edge in Toll-Venus during FLIP in NC 12 at the monitored regions. N=1 embryo.

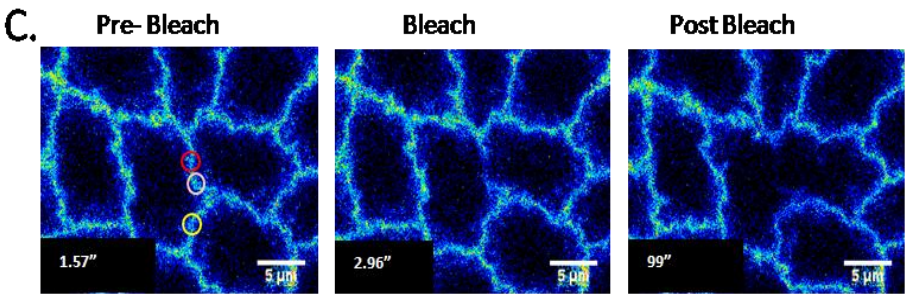

Fig.4.4 (C). Panel showing temporal mobility of Toll-Venus in pre-bleach (1.57"), bleach (2.96") and post bleach (99") images during FLIP in NC 13. Red and yellow regions indicate the ROI and the neighboring edge. Circle in light red shows the neighbor region on the same edge as ROI. -(with Bipasha Dey)

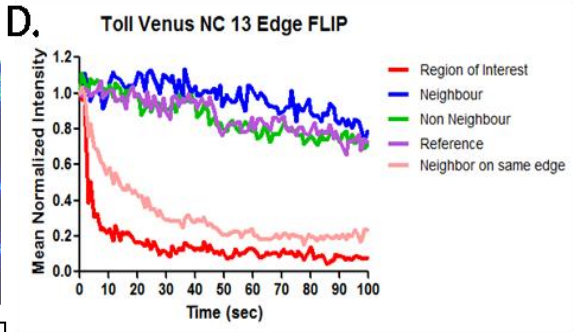

Graph. 4.4. (D). Temporal intensity distribution of an edge in Toll-Venus during FLIP in NC 13 at the monitored regions. N=1 embryo.

However, in cellularization, several rounds of bleaching over the ROI resulted in a drop in the intensity of both neighbor as well as non- neighbor edge. This drop was observed to continue till the intensity of both these regions got stabilized at a point (%) other than the ROI (Graph.4.4.F). The difference in stabilization of the monitored regions to distinct levels of intensity indicates the presence of diffusible and non-diffusible pool of Toll

Venus at this stage. The consistent decrease in intensity of the neighboring region within the same edge of the ROI was also observed during both syncytium and cellularization (light red line, Graph.4.4.F) which indicates that Toll diffuses freely within an edge but its movement is restricted across edges.

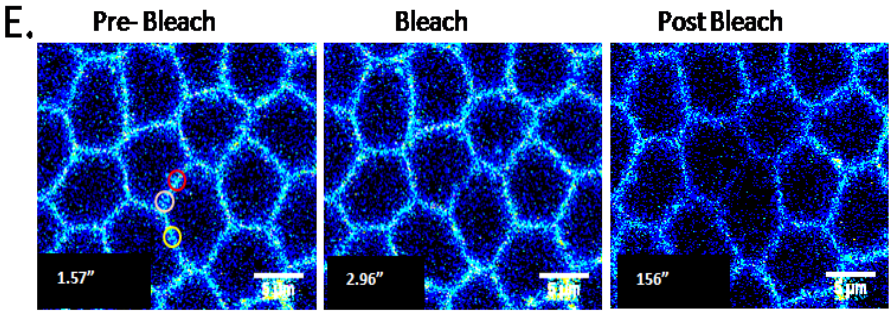

Fig.4.4 (E). Panel showing temporal mobility of Toll-Venus in pre-bleach (1.57"), bleach (2.96") and post bleach (156") images during FLIP in NC 14. Red and yellow regions indicate the ROI and the neighboring edge. Circle in light red shows the neighbor region on the same edge as ROI. (with Bipasha Dey).

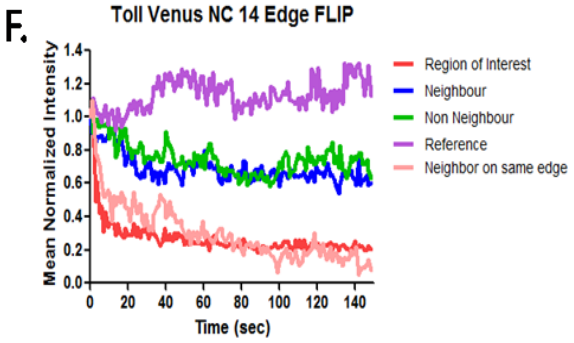

Graph.4.4. (F). Temporal intensity distribution of an edge in Toll-Venus during FLIP in NC 14 at the monitored regions. N=1 embryo.

II.c. Bazooka mobility in the plasma membrane

The extent of bleach during FRAP experiments on Bazooka GFP in NC 12-14 was 20% while the recovery was up to ~90%. In NC 12, the time taken for recovery of Bazooka GFP signal was ~35-45 seconds (Graph.4.5. B) and this duration became even less in NC 13 (~20-30 seconds) (Graph4.5.D)

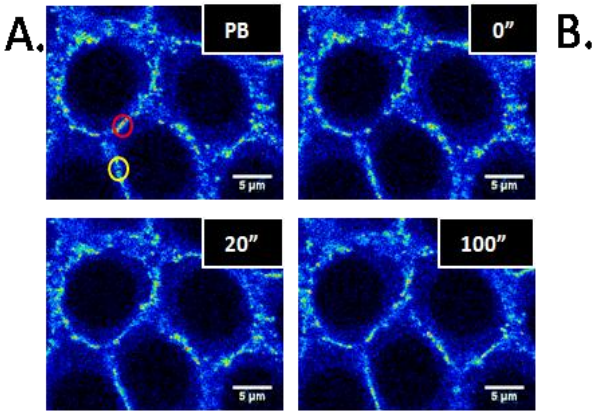

Fig.4.5 (A). Panel showing temporal mobility of Bazooka GFP in pre-bleach (PB), bleach (0'), half recovery (20") and full recovery (100") during FRAP in NC 12. Red and yellow regions indicate the ROI and the neighboring edge.

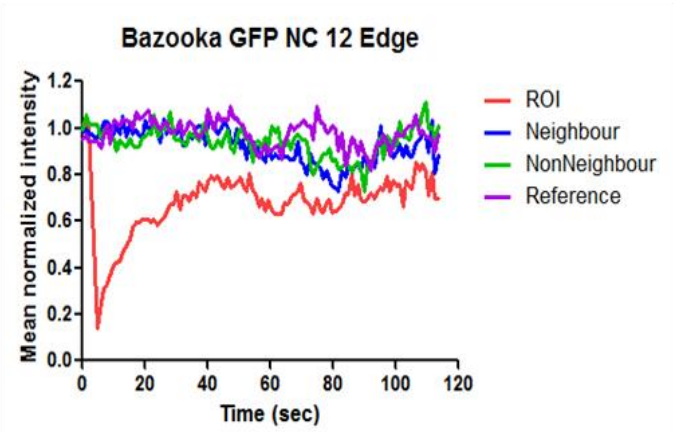

Graph.4.5 (B). Temporal intensity distribution on an edge during in Bazooka GFP FRAP in NC 12 at the monitored regions. N=1 embryo.

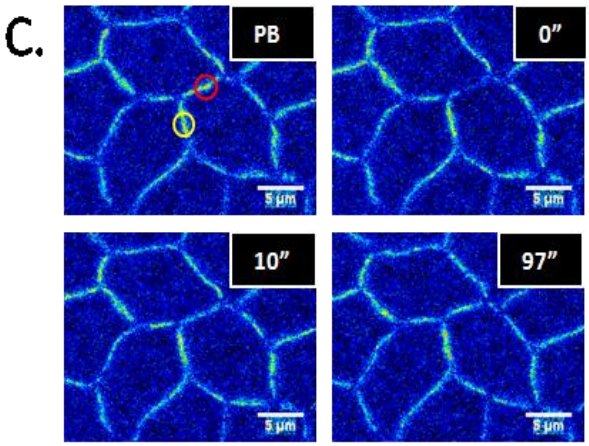

Fig.4.5(C). Panel showing temporal mobility of Bazooka GFP in pre-bleach (PB), bleach (0’), half recovery (10”) and full recovery (97”) during FRAP in NC 13. Red and yellow regions indicate the ROI and the neighboring edge respectively.

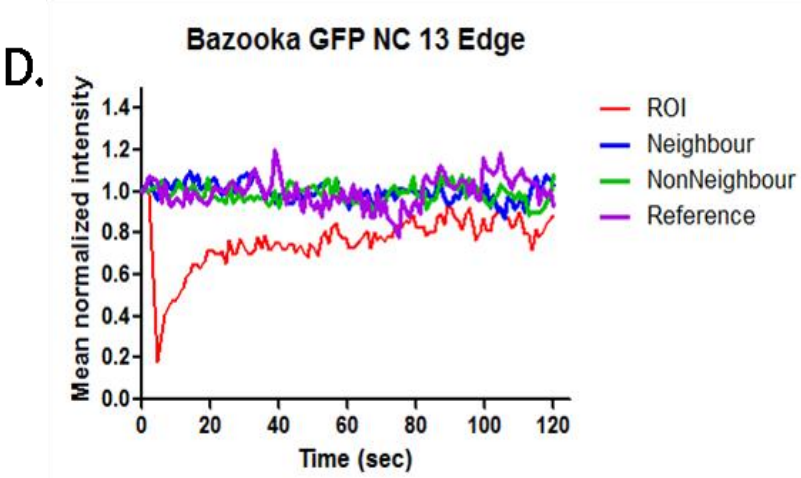

Graph.4.5 (D). Temporal intensity distribution of an edge in Bazooka GFP during FRAP in NC 13 at the monitored regions. N=1 embryo.

However during cellularization, it took ~70 seconds, longer than syncytium. And the fluorescence intensity of the neighbors as well as the non- neighbors were not observed to dip down during the respective time window of recovery in all division cycles (Graph.4.5.F).

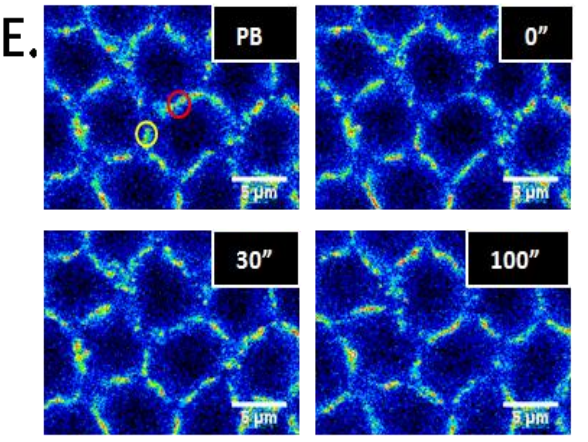

Fig.4.5 (E). Panel showing temporal mobility of Bazooka GFP in pre-bleach (PB), bleach (0’), half recovery (30”) and full recovery (100”) during FRAP in NC 14. Red and yellow regions indicate the ROI and the neighboring edge.

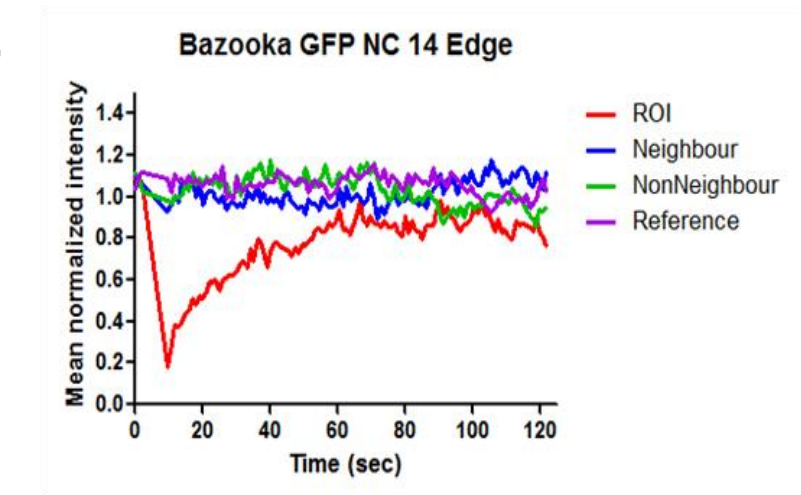

Graph.4.5.(F). Temporal intensity distribution of an edge in Bazooka GFP during FRAP in NC 14 at the monitored regions. N=1 embryo.

Corroborating the FRAP observations during syncytial division cycles, repeated bleaching of Bazooka GFP in the ROI did not show any depletion in the intensity of neighbors and non-neighbors although free diffusion was noticed from the neighbor region of the same edge (Graph.4.6.B,D).

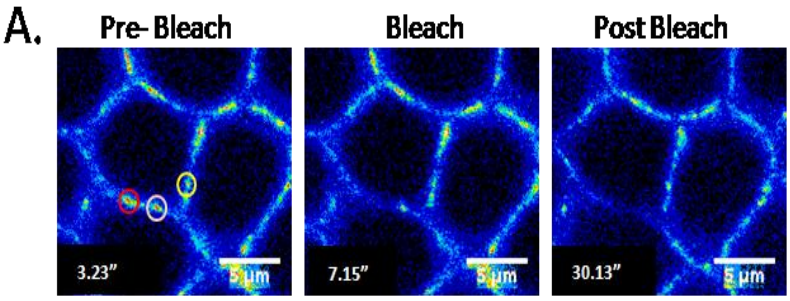

Fig.4.6(A). Panel showing temporal mobility of Bazooka GFP in pre-bleach (3.23"), bleach (7.15") and post bleach (30.13") images during FLIP in NC 12. Red and yellow regions indicate the ROI and the neighboring edge. Circle in light red shows the neighbor region on the same edge as ROI.

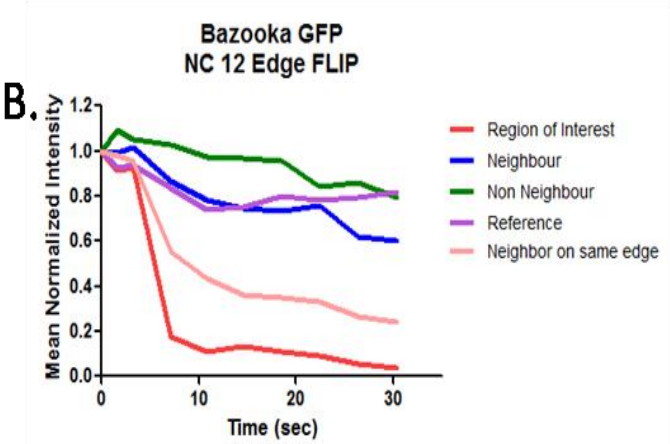

Graph.4.6.(B). Temporal intensity distribution of an edge in Bazooka GFP during FLIP in NC 12 at the monitored regions. N=1 embryo.

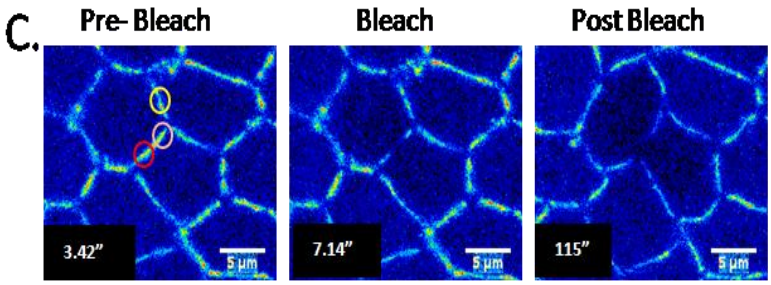

Fig.4.6 (C). Panel showing temporal mobility of Bazooka GFP in pre-bleach (3.42"), bleach (7.14") and post bleach (115") images during FLIP in NC 13. Red and yellow regions indicate the ROI and the neighboring edge. Circle in light red shows the neighbor region on the same edge as ROI.

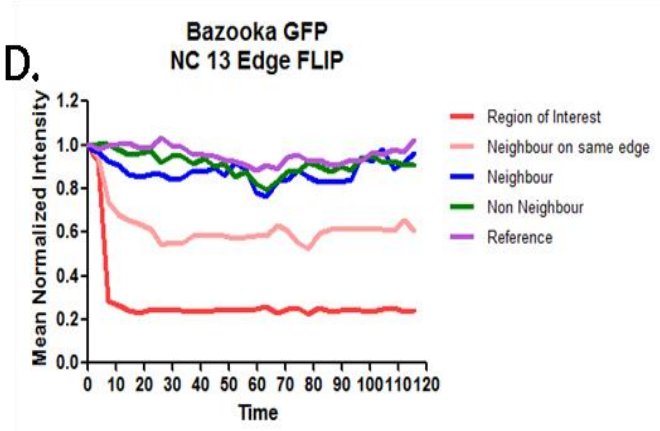

Graph.4.6. (D). Temporal intensity distribution of an edge in Bazooka GFP during FLIP in NC 13 at the monitored regions. N=1 embryo.

It is noticed that in NC 13, after a drop in intensity, the neighboring region on the same edge (light red line) shows a distinct level of stabilization of the intensity from ~30 seconds onwards in spite of the repeated bleaching of its adjacent region (ROI, the red line) (Graph.4.6.D). This indicates the existence of two different protein pools of Bazooka, probably one from the membrane itself and the other from the cytoplasm.

In cellularization, during FLIP, all the monitored regions other than the ROI, i.e., neighbors, non-neighbor and an unaffected region, were observed to have a decreasing trend in their fluorescent intensity signal (Graph.4.6.F) indicating overall intensity drop irrespective of photo bleaching.

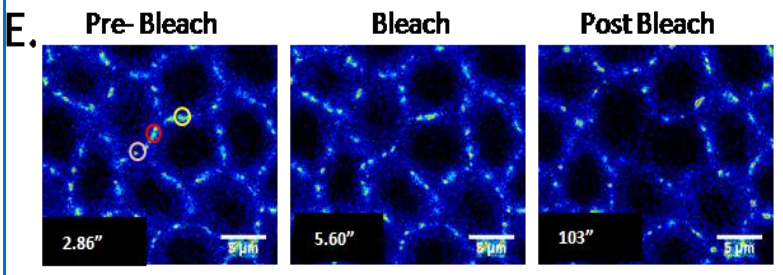

Fig.4.6 (E). Panel showing temporal mobility of Bazooka GFP in pre-bleach (2.86"), bleach (5.60") and post bleach (103") images during FLIP in NC 12. Red and yellow regions indicate the ROI and the neighboring edge. Circle in light red shows the neighbor region on the same edge as ROI.

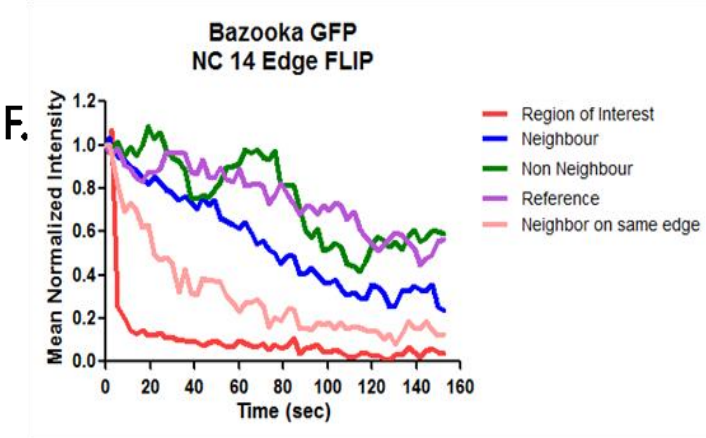

Graph.4.6. (F). Temporal intensity distribution of an edge in Bazooka GFP during FLIP in NC 14 at the monitored regions. N=1 embryo.

To summarize from the diffusion experiments, during syncytium, all three proteins, DE-Cadherin, Toll and Bazooka demonstrate compartmentalization of diffusion of molecules only within an edge of a polygonal pseudo epithelial cell.

The FRAP data analysis of DE-Cadherin GFP, Bazooka GFP and Toll Venus FRAP data is a representation from one sample across various cycles. Similarly, FLIP data analysis of all the above transgenic lines is a representation from one embryo only. However, same experiments were repeated across embryos and similar results have been obtained for multiple readings. A caveat to this analysis of diffusion experiments is the all the proteins in the study have been genetically over expressed in the embryos. So, the behavior of diffusion is a reflection of the movement of over expressed protein pool, which might be different from the endogenous one. However, the fact that we observe differential mobility in different cycles implies that PM or protein dynamics are changing with the same reporter. Over-expressed line of Bazooka GFP is shown to rescue *Bazooka* mutants indicating the dynamics of the over expressed pool should be similar to the endogenous one. And in case of Cadherin, we plan to study its dynamics

in transgenic Endo-DE-Cadherin embryos in which GFP is fused with endogenous Cadherin.

III. Studying the plasma membrane organization in *Cadherin (shg^{6115})* mutants during syncytium.

Which comes first- Junctions or plasma membrane polarization? Do Adherens Junctions (AJs) form in the syncytial PM and do they form prior to a polarized membrane formation? In an attempt to find answers regarding the mechanism behind polarized organization of proteins in the syncytial plasma membrane, we tried to characterize the plasma membrane organization in the absence of the component of AJ (Cadherin) during this crucial time window of inception of PM polarity. Following this up, loss of function mutations in Cadherin were generated by a combination of *wimp* and *Cadherin* hypo orphic mutants.

III. a. Embryonic lethality of *shg^{6115}* mutant embryos

100 embryos each, from 3 separate collections were counted over 48 hours to obtain the percentage of embryonic lethality in the loss-of-function mutants of Cadherin. The embryonic lethality was 23.6%.

III.b. Depleted level of Cadherin in *shg^{6115}* embryos as compared to the control

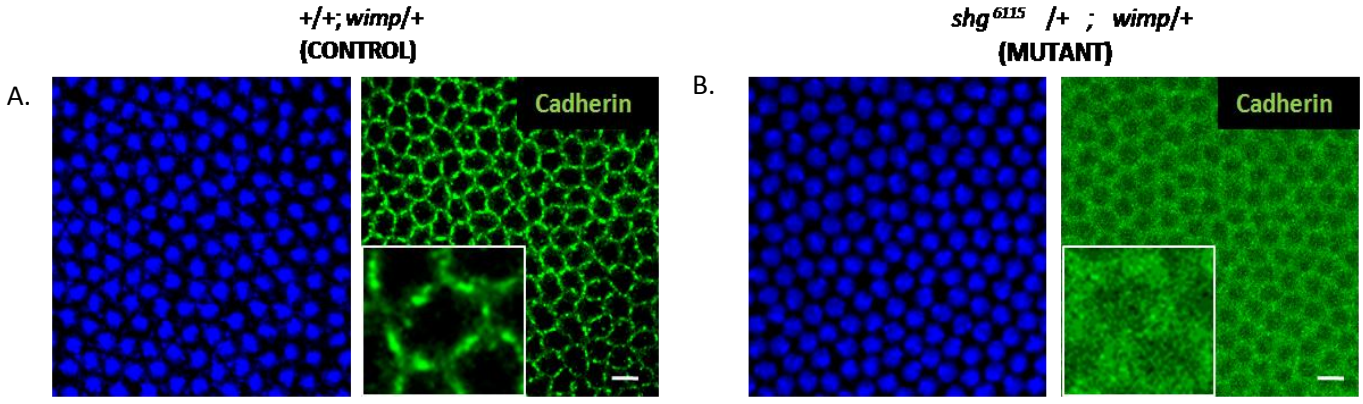

Fig.5.1. Panel (A) shows Anti Cadherin immuno-staining (green) on the plasma membrane and DNA labeled with DAPI (in blue) in NC 14 of the control embryos. Panel (B) shows the loss of Anti- Cadherin staining on the plasma membrane in loss of function Cadherin mutant embryos. Insets show magnified PM organization stained by Anti-Cadherin. Scale bar: 5µm.

Anti-Cadherin staining on the PM is absent in the mutant indicating that the level of Cadherin is reduced in the *shg*^{6115} embryos as compared to the control (Fig.5.1).

III.c. Shallow plasma membrane architecture and failure of metaphase furrow ingression during syncytium in *Cadherin* mutants

As a result of decrease in levels of Cadherin in the mutant embryos, starting from NC 11 till NC 13, loose membrane architecture was observed in each of these division cycles when stained by membrane marker Amphiphysin (green panel). Shallow membrane is indicated by red arrows in Fig.5.2 and Fig.5.2 where the missing portions are only apically present and hence is missing in the lateral domain.

The ingressing lateral membrane during metaphase of every nuclear cycle seem to be seem to be affected in the mutant. In NC 11, loop-like structure are observed (red arrow on saggital section of panel B in Fig.5.2). Their extent of ingression is less when compared to the control as seen in NC 12 (white line on saggital section of panel B in Fig.5.3). Moreover, the direction of this ingression is also tilted at an angle instead of pointing straight downward (white arrows on saggital section of panel B in Fig.5.3). The mean length of the ingressing membrane in the control saggital section is 9.14 µm while the mutant lateral membrane length is only 5.30 µm. However, this observation of shortened membrane length is only observed in few embryos at NC 12 and NC 13.

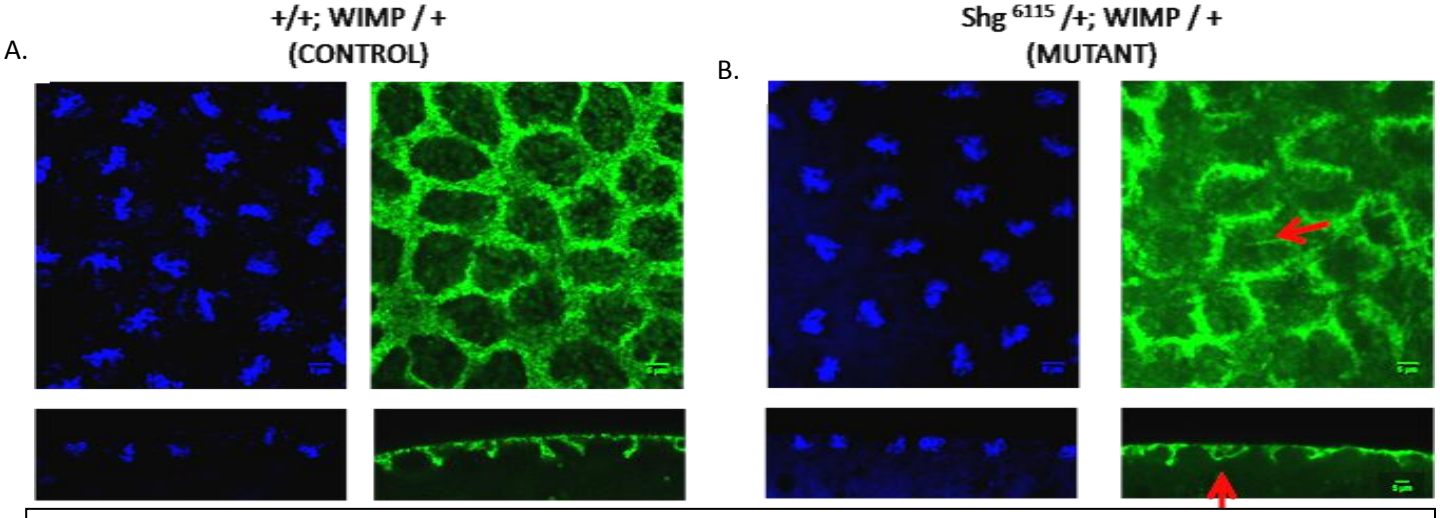

Fig.5.2. Panels (A) shows plasma membrane organization labeled with Amphiphysin (in green) and DNA labeled with DAPI (in blue) in NC11 metaphase membrane of control embryos. Sections below represent the corresponding saggital sections. Panel (B) shows the membrane organization in loss of function Cadherin mutants. Red arrow in the cross section indicates discontinuity in the membrane and the one in the saggital section points to the loop like invaginations of the lateral membrane. Scale bar: 5µm.

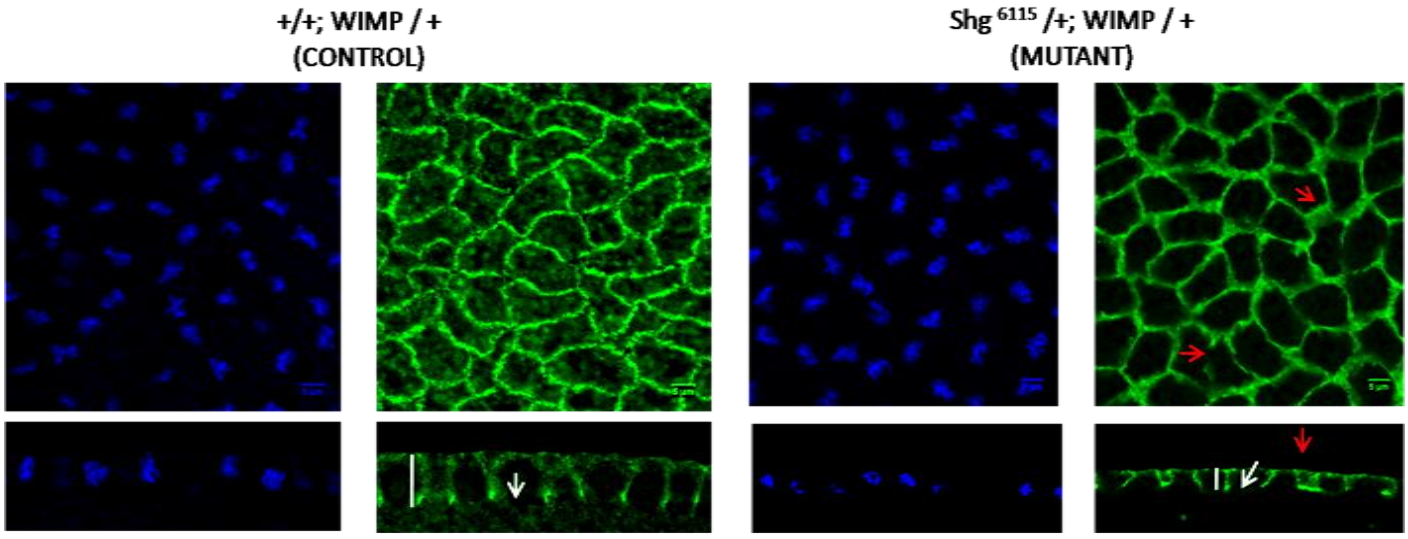

Fig.5.3. Left panels shows plasma membrane organization labeled with Amphiphysin (in green) and DNA labeled with DAPI (in blue) in metaphase NC12 of control embryos. Right panel shows the membrane organization in loss of function Cadherin mutants. Saggital sections are present below the corresponding cross sections.

Red arrow in the mutant membrane cross section indicates loose architecture and the one in the saggital section points to the loop like invaginations of the lateral membrane. The white straight line indicates the length of metaphase lateral membrane, while the white arrow shows the direction of ingression in both control and mutant embryos. Scale bar: 5 µm.

III.d. Packing of the epithelial cells in terms of polygonal shapes is affected in the *Cadherin* mutants during syncytium.

Previous lab studies show epithelial cell packing in NC 12 with a balance between five, six and seven sided polygons where hexagons are the most predominant ones (Graph.5.1.B). As compared to this, the packing that comes up during syncytium in the *shg*^{6115} mutants demonstrate more number of four and five sided polygons in NC 12 and 13, with pentagons being the most frequent one (Graph.5.1.C).

A.

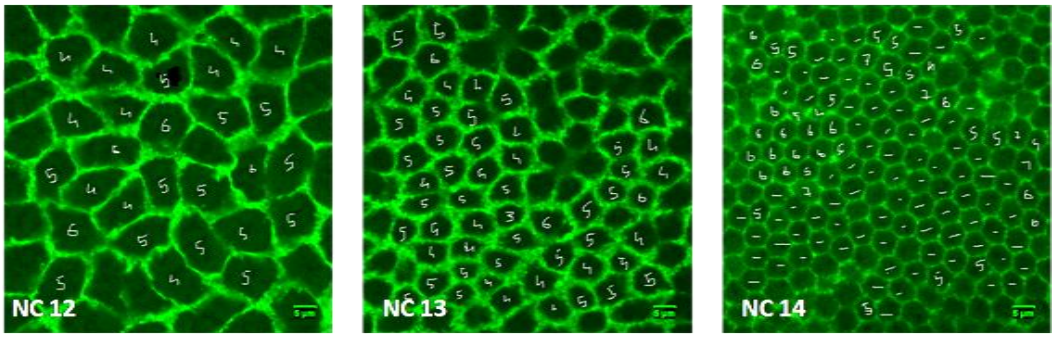

Fig.5.4 (A). Representative image sections of PM for manual polygon counting from NC12 to NC 14 in Cadherin mutants.

B.

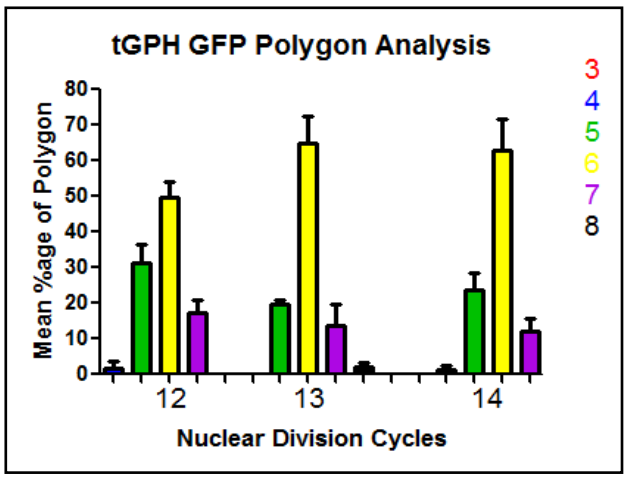

Graph.5.1 (B). Distribution of N-sided polygons in nuclear cycles 12 -14 in tGPH labeled plasma membrane organization. N=3 embryos.

C.

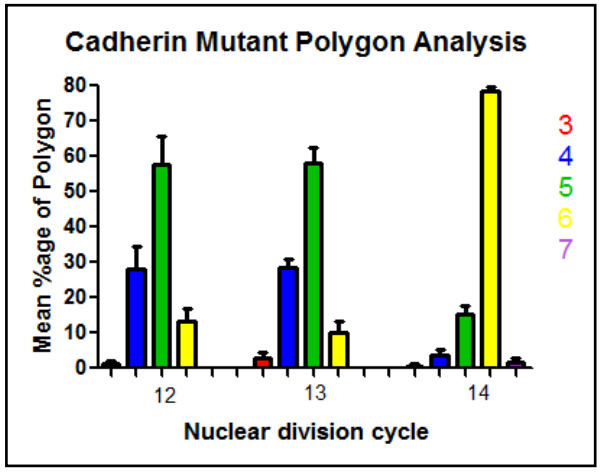

Graph.5.1(C). Distribution of N-sided polygons in NC 12-14 of plasma membrane organization in the Cadherin mutant labeled with membrane marker Amphiphysin. N=3 embryos.

IV. Studying the plasma membrane organization in *Bazooka (baz^{19A})* mutants

In order to understand the mechanism behind the PM polarity on the lateral domain, in addition to *Cadherin* mutants, loss-of-function mutants of Bazooka were also generated to disrupt its asymmetric distribution mostly enriched in the edges. The integrity of the plasma membrane architecture as well as pattern of polygonal packing is looked at in this mutant.

IV. a. Embryonic lethality of *baz^{19A}* mutants

100 embryos each, from 3 separate collections were counted over 48 hours to obtain the percentage of embryonic lethality in the loss-of-function mutants of *Bazooka*. The embryonic lethality was above 80%.

IV. b. Depleted levels of Bazooka in *baz^{19A}* mutant embryos

Level of Bazooka is reduced in the *baz^{19A}* embryos when compared to the control (Fig.5.5) as seen by the loss of Anti-Bazooka staining in the *Bazooka* mutant embryos.

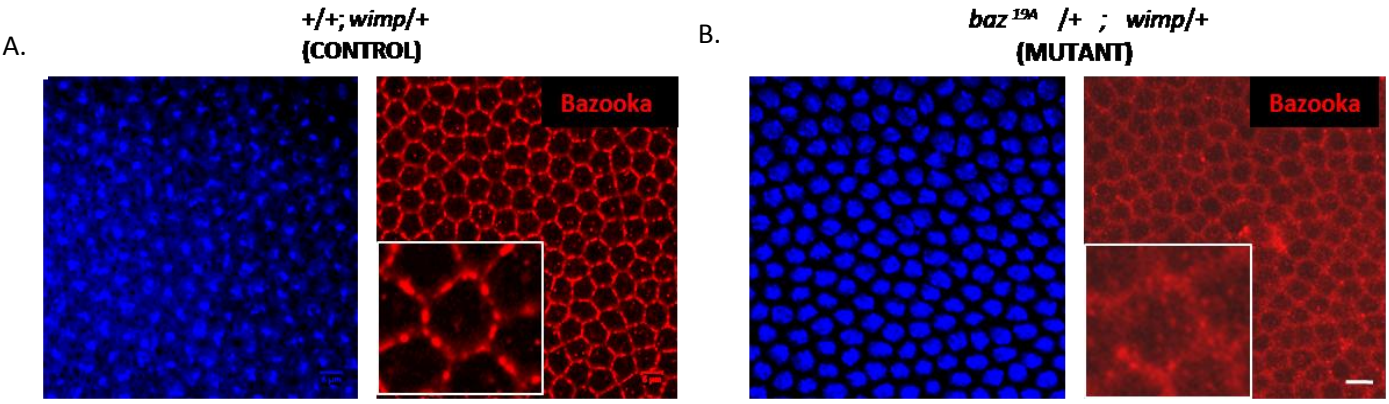

Fig.5.5. Panel (A) shows Anti Bazooka immuno-staining (red) on the plasma membrane and DNA labeled with DAPI (in blue) in NC 14 of the control embryos. Panel (B) shows the loss of Anti- Bazooka staining on the plasma membrane in loss of function Bazooka mutant embryos. Insets show magnified PM organization stained by Anti-Bazooka. Scale bar: 5µm.

IV.c. Broad plasma membrane architecture in *baz*^{19A} mutant embryos during syncytium

During NC 13, the *Bazooka* mutant embryos in mid-metaphase stained with membrane marker shows loose and broad membrane architecture as compared to the *wimp* control in prophase where the membrane is tight (Fig.5.6).

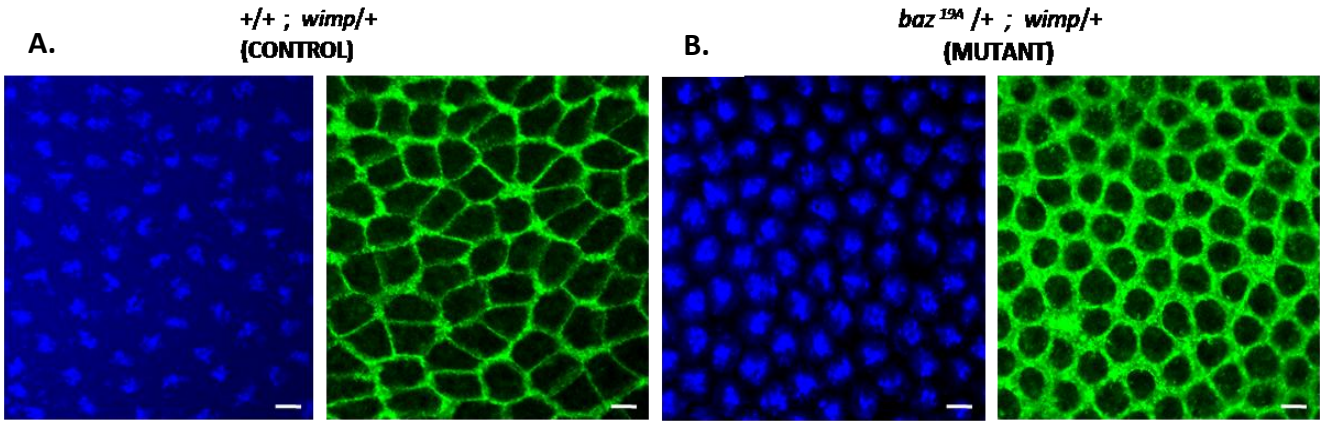

Fig.5.6. Panel (A) shows Anti Amphiphysin immuno-staining (green) on the plasma membrane and DNA labeled with DAPI (in blue) in NC 13 of the wimp control embryos. Panel (B) shows the broader Anti-Amphiphysin staining on the plasma membrane in loss of function Bazooka mutant embryos. Scale bar: 5µm.

IV.d. Packing of the epithelial cells in terms of polygonal shapes is affected in the *Bazooka* mutants during syncytium.

The balance in terms of polygons mostly between pentagons, hexagons and heptagons, as observed in tGPH GFP, shifts towards tetragons, pentagons, hexagons in baz^{19A} mutant embryos with pentagons being the most frequent one (Fig.5.7) for baz^{19A} embryo images). This trend in packing is observed in both syncytium (NC 12, 13) and cellularization (NC 14) in contrast to the packing observed in tGPH GFP (Graph.5.2).

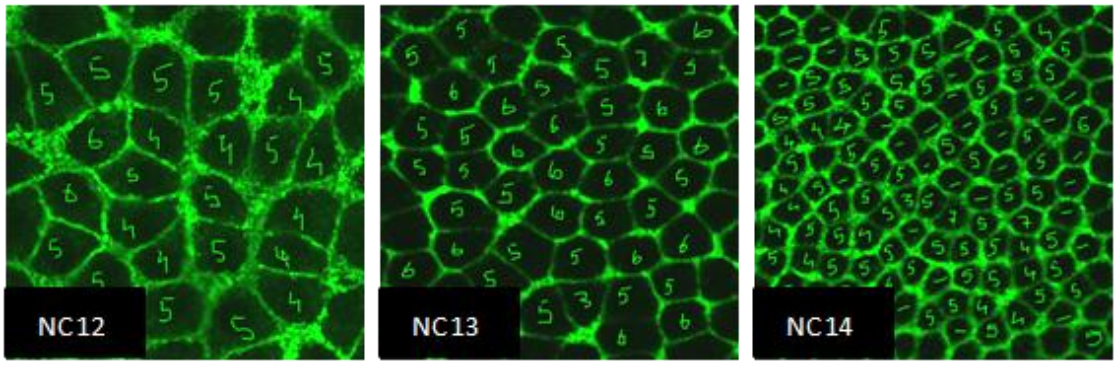

Fig.5.7. Representative image sections of PM for manual polygon counting from NC12 to NC 14 in Bazooka mutants labeled with membrane marker PatJ.

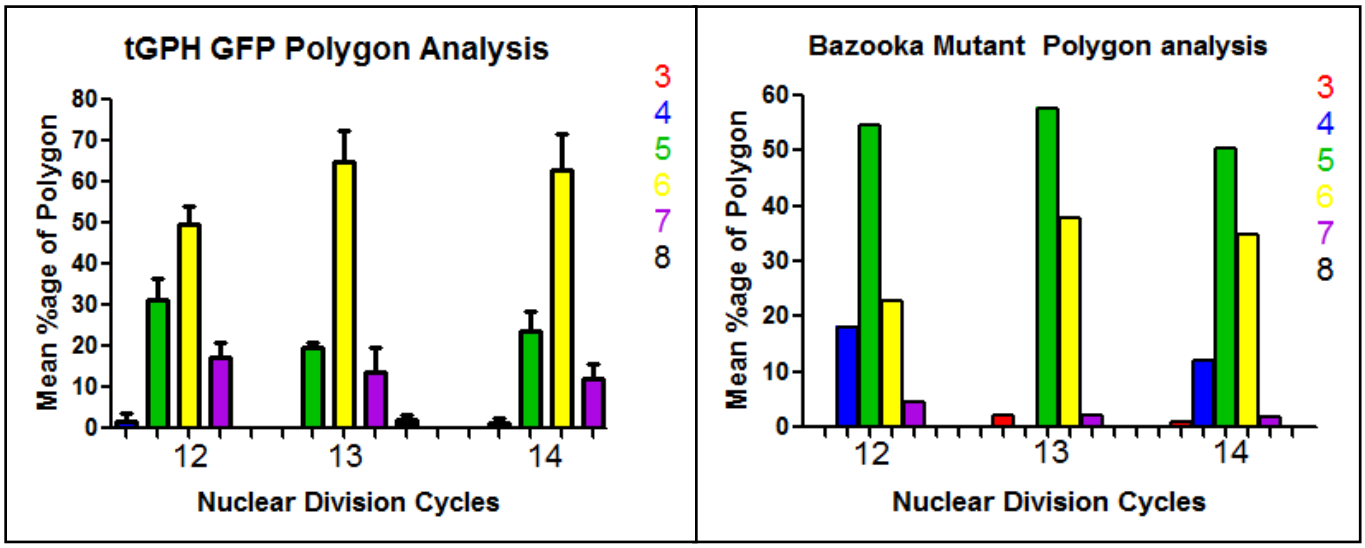

Graph.5.2. Distribution of N-sided polygons in NC 12-14 of plasma membrane organization in the tGPH GFP and Bazooka mutant embryos. N= average of 2 embryos for Bazooka mutant.

IV.e. Disruption of XY polarity of the lateral membrane in terms of Peanut localization across edges and vertices in *Cadherin* and *Bazooka* mutants.

The asymmetric distribution of Peanut is affected in both *Cadherin* and *Bazooka* mutant embryos. It is more on edges of the PM in mutant embryos as compared to that in the wild type embryos (Fig.5.8).

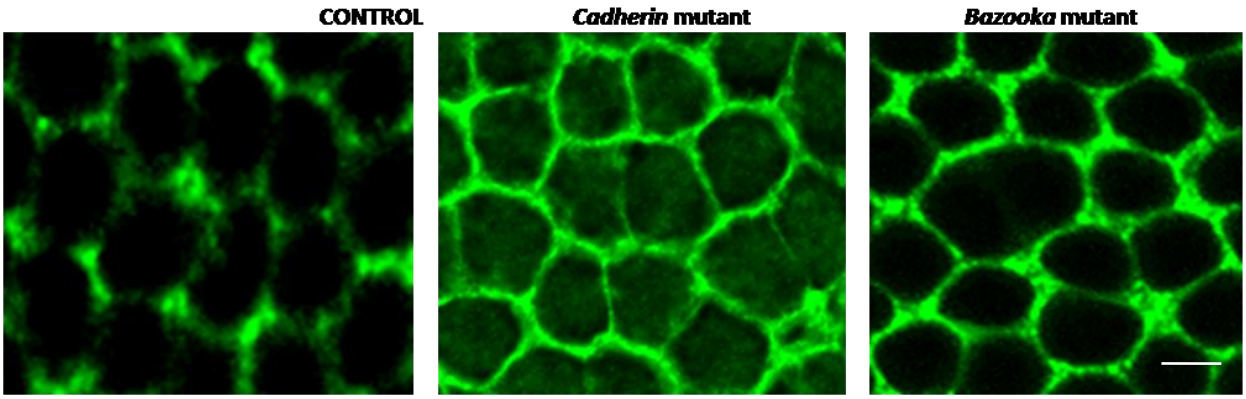

Fig.5.8. Panel shows Anti-Peanut staining on the plasma membrane of control, shg^{6115} and baz^{19A} embryos (from left). Cadherin and Bazooka mutants show loss of polarized localization of Peanut only in vertices. Scale bar:- 5µm.

In terms of intensity measurement, vertex is almost 2-fold brighter than an edge of the polygonal epithelial cells in a wild type embryo. But in *Cadherin* and *Bazooka* mutants, the difference in intensity measurement between edges and vertices becomes very less with approximately uniform distribution all over (Graph.5.3).

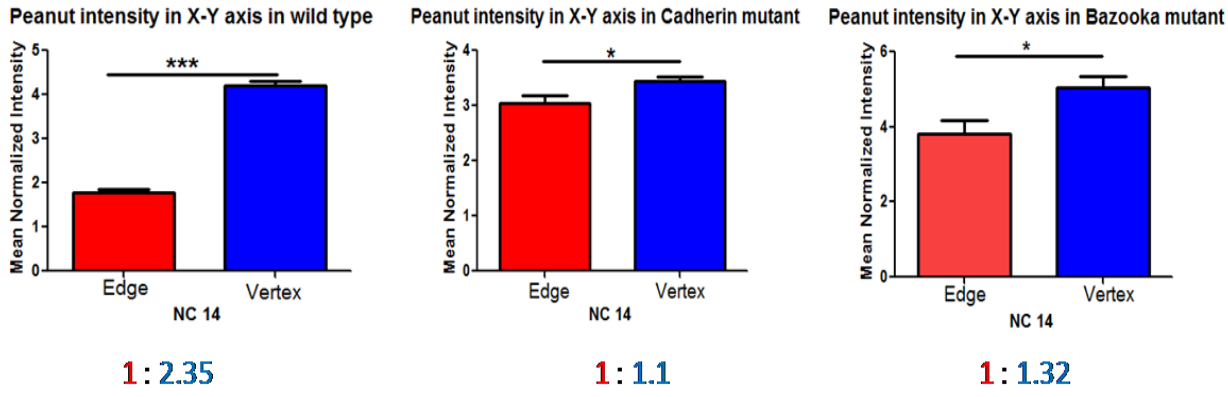

Graph.5.3. *Mean normalized intensity across edges and vertices of the PM labeled with Anti-Peanut in* control, *shg^{6115}* and *baz^{19A} embryos in NC 14. p<0.05=*, p<0.001=***. N=15 edges/vertices in 1 embryo.* The ratios below each bar graph represent the difference in intensity across edge vs. vertex.

Discussion

Plasma membrane polarity is established during syncytial mitosis in both X - Y and X - Z axis.

Previous studies on polarity of the PM have already demonstrated the existence of 2 lateral domains and an apical domain in X-Z axis during syncytium, with respect to certain proteins. This report adds on yet another dimension that is, in X-Y axis to their polarized distribution across edges (Bazooka) and vertices (Septins) from NC 12 onwards (as shown in Fig.6.1). One might ask: how do these proteins get such a polarized location? During syncytial cycles, most of the polarity as well as cytoskeletal remodeling proteins are known to form de novo as well as redistribute to some extent, indicating that these proteins clearly have some directed pathway to get them docked onto the PM. Although the mechanism is not yet known, this might be due to compartmentalization of molecules even in the absence of complete epithelial cell during syncytium. And what is the functional relevance of such a pattern? To this end, there are reports on Septins, indicating that it polymerizes to form filamentous structures that act as diffusion barriers between PM domains (Nelson, 2006). Hence, more Septins at the vertices of the polygonal organization might imply its role in restricting diffusion of molecules across edges via vertices

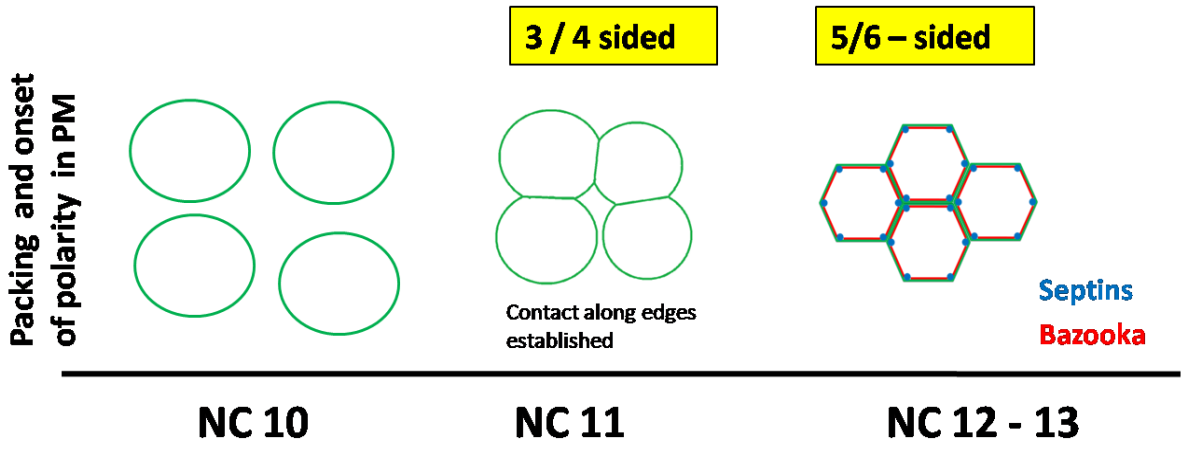

Fig.6.1. Schematic of the packing and polarized distribution of proteins on the polygonal architecture of the PM along X-Y axis during NC 10-14. ***tGPH,*** ***Bazooka,*** ***Septins*** *are represented in green, red, blue respectively.*

The edge of a polygon is a compartment in the syncytium: Cadherin and Toll are mobile within one edge and do not traverse the vertex

From photo bleaching experiments, Cadherin molecules in syncytium, seem to be restricted in terms of their movement only within a single edge of an incomplete epithelial cells, with no contribution from the neighboring edge during recovery. Cadherin, being a cell-cell adhesion protein, the lack of contribution of proteins from the neighboring edge might imply that the zipping of the Cadherin molecules with one another prevents their free movement. However, this kind of homophillic interactions of Cadherin molecules in the syncytium is not well characterized. To test this hypothesis, one can use calcium chelating agents to disrupt the adhesion of homophilic Cadherin molecules and then follow the Cadherin mobility pattern across edges.

In spite of the protein pool of Cadherin being depleted to its steady state minimum during FLIP, no change in the intensity profile of the neighboring edges indicates that there exists no threshold for Cadherin molecules from there to diffuse. This phenomenon seems to arise exclusively because of compartmentalization (Fig.6.2). The property, however, is not unique to only Cadherin since another trans-membrane protein, Toll also demonstrates such a trend of restricted diffusion. What might be different are the distinct pools of diffusible fraction of molecules that contribute to the recovery. There are mainly two possibilities: either it gets recovered from the redistribution of the remaining molecules of the same edge or proteins from the cytoplasm get docked on the PM, thus contributing to the recovery.

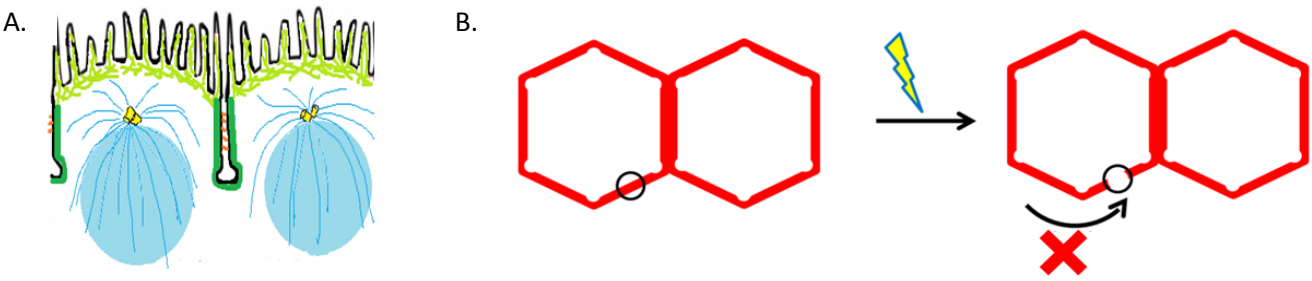

Fig.6.2. Schematic for diffusion of molecules during syncytium when PM is not completely formed. Panel A shows incomplete PM ingression in syncytium and Panel B shows diffusion (for Cadherin, Toll and Bazooka) restricted only within an edge.

Differential mobility of Toll, Cadherin and Bazooka in the syncytial plasma membrane

In contrast to diffusion of Cadherin which takes constant time to recover after photo bleaching in every division cycle, Toll and Bazooka demonstrates a trend of faster recovery in NC 12-13. This might imply that Toll and Bazooka molecules are more mobile than Cadherin and hence diffuses faster. For each protein, faster recovery across different nuclear cycles seems to be due to an increase in protein pool contributing to the same fixed area being bleached with every division.

During cellularization, the intensity dip in the neighboring and the non-neighboring edges during repeated photo bleaching of Toll-Venus is due to redistribution of proteins over the newly formed PM. This is in contrast to Cadherin which seems to get redistributed only within an edge in NC 14. However, the neighboring and the non-neighboring edge getting stabilized to a different point in Toll Venus FLIP experiments indicates existence of two different diffusible pools which might contribute to the bleached ROI.

During cellularization, photo bleaching experiments with Bazooka GFP, in case of FRAP, shows slow recovery compared to recovery time during syncytium. This might be due to the distribution of the bazooka itself, it appears to be in the form of multiple punctae in NC14 as compared to the tight and uniform distribution of Bazooka over a single edge during NC 12 and 13. And in FLIP experiment, intensity of all the monitored regions is found to decrease which is due to the overall dip in intensity of the fluorescent molecules at that plane during this phase irrespective of photo bleaching. Previously, it is known that syncytial PM has Bazooka in the baso-lateral domain, which later on gets transported to the sub apical domain during cellularization (Harris and Peifer, 2005). It is speculated that the time window of FLIP experiment coincides with this baso-lateral to apical shift in localization of Bazooka. But, the fact that the neighboring edge intensity decreases more than the non-neighbor and the reference edge might imply its contribution to the bleached area.

Cadherin mutant embryos show shallow and compromised lateral membrane

Shallow PM architecture might arise as a result of minimal adhesion between the PM of the adjoining cells in the epithelial cell sheet. If true, this directly points out that Cadherin achieves it property of adhesion already in syncytium. Moreover, the compromised length and tilted invagination of the metaphase furrow implies that Cadherin has an important role in both stabilizing and directing the ingression of the lateral domain of PM.

Bazooka mutant embryos show broad architecture of the lateral membrane domain

During cellularization, Bazooka is known to interact with Cadherin, its downstream effector in establishing junction-dependent epithelial cell polarity (Harris and Pfeifer, 2004). From this loss-of-function *Bazooka* mutant PM architecture, it seems that the interaction between Bazooka and Cadherin is established at syncytium itself since depleted levels of Bazooka gives rise to looseness and destabilization in the lateral membrane which, in turn, might arise due to less Cadherin on the membrane. It also hints at the fact that Bazooka functionally helps in getting cells adhere to each other tightly even when the complete PM is not formed. To this end, we further need to stain the embryos against DE-Cadherin antibody and look for its localization in the syncytial embryos. Like *Cadherin* mutant embryos, to check whether the membrane ingression is also compromised in *Bazooka* mutants, more immuno-staining of both the control as well as the mutant embryos need to be done against a membrane marker in the metaphase stage of syncytial division cycles and the length of membrane ingression in both cases needs to be compared.

Polygonal distribution pattern is altered in both _Cadherin_ and _Bazooka_ mutants during syncytium

Less interaction of Cadherin with the actomyosin network via cytoplasm linkers leads to instability of adherents junctions which might affect the F-actin localization to the apical domain in the *Cadherin* mutant embryos. Packing of PM between nuclei is possibly governed by the interplay between the nuclear array in the syncytium and F-actin in the

caps (Kanesaki et al., 2011). And hexagonal packing involves adhesion and junction remodeling, which is believed to be modulated by E-Cadherin dynamics in epithelial cells (Cavey et al., 2008). Supporting this point of view, compromised cell-cell adhesion again might be reason behind the predominance of pentagons instead of hexagons in the mutant scenario. In addition since Bazooka seems to interact with Cadherin from syncytium onwards, depleting Bazooka also might indirectly affect Cadherin localization, which might lead to the shift in balance more towards pentagons instead of hexagons in *Bazooka* mutants.

Future prospects

Septins, as mentioned earlier, acts as diffusion barriers in PM domains. Since its distribution is more on the vertices, it will be interesting to carry out the diffusion experiments of the compartmentalized proteins like Cadherin, Toll in the loss-of-function mutants of Sep2 or Peanut during syncytial division cycles. Free movement of molecules from neighboring edge to the bleached region after photo bleaching would directly indicate the functional relevance of polarized Septin localization on vertices.

The question that is still remains unexplored is: What is the functional utility for such a unique feature of compartmentalized movement just within an edge at such an early embryonic stage without the formation of complete epithelial cells?

To gain deeper insights into the functional relevance of adhesion junctions in the initiation of polarity in PM organization, we need to more systematically characterize the distribution of other proteins present in the lateral domain of the PM along and X-Z axis in loss-of-function mutants of *Cadherin* and *Bazooka.* Elucidating more on the mechanism of this inception of polarity, it would be also interesting to look at the role of cytoskeletal remodeling proteins like Peanut in PM architecture formation.

References

Assémat, E., Bazellières, E., Pallesi-pocachard, E., Bivic, A. Le, and Massey-harroche, D. (2008). Polarity complex proteins. Biochimica et Biophysica Acta *1778,* 614-630.

Brand, A.H., and Perrimon, N. (1993). Targeted gene expression as a means of altering cell fates and generating dominant phenotypes. Development *415*, 401–415.

Cavey, M., Rauzi, M., Lenne, P.-F., and Lecuit, T. (2008). A two-tiered mechanism for stabilization and immobilization of E-cadherin. Nature *453*, 751–756.

Ellenbroek, S.I.J., Iden, S., and Collard, J.G. (2012). Cell polarity proteins and cancer. Seminars in Cancer Biology *22*, 208–215.

Fischer, J.A., Giniger, E., Maniatis, T., and Ptashne, M. (1988). Gal4 activates transcription in Drosophila. Nature 332:853-856.

Founounou, N., Loyer, N., and Borgne, R. Le (2013). Article Septins Regulate the Contractility of the Actomyosin Ring to Enable Adherens Junction Remodeling during Cytokinesis of Epithelial Cells. Developmental Cell *24*, 242–255.

Frescas, D., Mavrakis, M., Lorenz, H., Delotto, R., and Lippincott-schwartz, J. (2006). The Journal of Cell Biology: Article. *173*, 219–230.

Gibson, M.C., and Ã, N.P. (2003). Apicobasal polarization: epithelial form and function. Current Opinion in Cell Biology. 747–752.

Harris, T.J.C., and Peifer, M. (2004). Adherens junction-dependent and -independent steps in the establishment of epithelial cell polarity in *Drosophila*. The Journal of Cell Biology *167*, 135–147.

Harris, T.J.C., and Peifer, M. (2005). The positioning and segregation of apical cues during epithelial polarity establishment in *Drosophila*. The Journal of Cell Biology. *170*, 813–823.

Kanesaki, T., Edwards, C.M., Schwarz, U.S., and Grosshans, J. (2011). Dynamic ordering of nuclei in syncytial embryos: a quantitative analysis of the role of cytoskeletal networks. Integrative Biology: Quantitative Biosciences from Nano to Macro. 3, 1112–1119.

Lecuit T, Wieschaus E. (2000). Polarized insertion of new membrane from a cytoplasmic reservoir during cleavage of the *Drosophila* embryo. The Journal of Cell Biology *150*, 849-860.

Mavrakis, M., and Rikhy R., Lippincott-Schwartz, J. (2009). Plasma membrane polarity and compartmentalization are established before cellularization in fly embryo. Developmental Cell. *16*, 93–104.

Mavrakis, M., Rikhy, R., and Lilly, M. (2008). Fluorescence Imaging Techniques for Studying *Drosophila* Embryo Development. Current Protocols in Cell Biology. 4.18.1-4.18.43.

Munro, E., Nance, J., Priess, J.R., and Harbor, F. (2004). Cortical Flows Powered by Asymmetrical Contraction Transport PAR Proteins to Establish and Maintain Anterior-Posterior Polarity in the Early C . elegans Embryo. Developmental Cell *7*, 413–424.

Neganova, I.E., Sekirina, G.G., and Eichenlaub-ritter, U. (2000). Surface-expressed E-cadherin , and mitochondrial and microtubule distribution in rescue of mouse embryos from 2-cell block by aggregation. *6*, 454–464.

Orlando, K., and Guo, W. (2009). Membrane Organization and Dynamics in Cell Polarity. Cold Spring Harbor Perspectives in Biology. *1–17.*

Parkhurst S,M, Horowicz. D,I. (1991). wimp , a dominant maternal-effect mutation , reduces transcription of a specific subset of segmentation genes in *Drosophila*. Genes and Development. *5,* 341–357.

Petricka, J.J., Norman, J.M. Van, and Benfey, P.N. (2009). Symmetry Breaking in Plants: Molecular Mechanisms Regulating Asymmetric Cell Divisions in Arabidopsis. Cold Spring Harbor Perspectives in Biology, 1–17.

Pinal, N., Goberdhan, D.C., Collinson, L., Fujita, Y., Cox, I.M., Wilson, C., Pichaud, F. (2006). Regulated and polarized PtdIns(3,4,5)P3 accumulation is essential for apical membrane morphogenesis in photoreceptor epithelial cells. Current Biology *16,* 140–149.

Rose, L.S., and Kemphues, K.J. (1998). EARLY PATTERNING OF THE C . ELEGANS EMBRYO.

Rabut, G. and Ellenberg, J. (2005). Photobleaching techniques to study mobility and molecular dynamics of proteins in live cells: FRAP, iFRAP, and FLIP. In Live Cell Imaging: A Laboratory Manual. (R.D.Goldman and D.L. Spector, eds.) pp. *101-126.* Cold Spring Harbor Laboratory Press, Cold Spring Harbor, N.Y

Rothwell, W.F., and Sullivan, W. (2007). *Drosophila* Embryo Collection. Cold Spring Harbor Protocols, pdb.prot4825.

Sherlekar, A, and Rikhy, R. (2011). "*Drosophila* embryo syncytial blastoderm cellular architecture and morphogen gradient dynamics: Is there a correlation?" Review Literature And Arts Of The Americas: 1-10

Sokac, A.M., and Wieschaus, E. (2008). Zygotically controlled F-actin establishes cortical compartments to stabilize furrows during *Drosophila* cellularization. The Journal Of Cell Science *121*, 1815-1824.

Spiliotis ET, Nelson WJ. (2006). Here come the septins: novel polymers that coordinate intracellular functions and organization. The Journal of Cell Science.; *119*:4–10.

St Johnston, D., and Ahringer, J. (2010). Cell polarity in eggs and epithelia: parallels and diversity. Cell *141*, 757–774.

Thomas, G.H., and Williams, J.A. (1999). Dynamic rearrangement of the spectrin membrane skeleton during the generation of epithelial polarity in *Drosophila*. The Journal of Cell Science *2852*, 2843–2852.

Wodarz, A. (2005). Molecular control of cell polarity and asymmetric cell division in *Drosophila* neuroblasts. Current Opinion in Cell Biology *17*, 475–481.

Wodarz, A., Ramrath, A., Grimm, A., and Knust, E. (2003). *Drosophila* Atypical Protein Kinase C Associates with Bazooka and Controls Polarity of Epithelia and Neuroblasts. The Journal Of Cell Biology *150*, 1361–1374.

Yuki, T, Hiroyuki Y, Yumiko A, Yoshinori S, Shintaro I. (2013). Activation of TLR2 Enhances Tight Junction Barrier in Epidermal Keratinocytes" The Journal of Immunology. doi:10.4049/jimmunol.1100058.